Surface Parameter Estimation: Basics and Advanced Concepts

Irena Hajnsek

Earth Observation and Remote Sensing

Chair of Earth Observation and Remote Sensing
Institute of Environmental Engineering, ETH Zürich
Microwaves and Radar Institute, DLR Oberpfaffenhofen

DLR

Overview

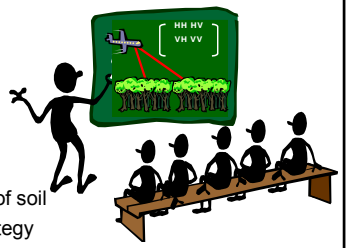

Part I: Theory and basics

- Introduction into SAR polarimetric observables
- Decomposition techniques
- Introduction into material properties of soil
- Model description and inversion strategy

Part II: Exercises with L-band airborne data

- Read the data
- Speckle filtering
- Oh, Dubois and X-Bragg inversion

DLR

Motivation of Radar Remote Sensing

- **Independent from Weather**
  - *Data acquisition during cloud cover, rain, ...*
- **Radar is complementarily to optics**

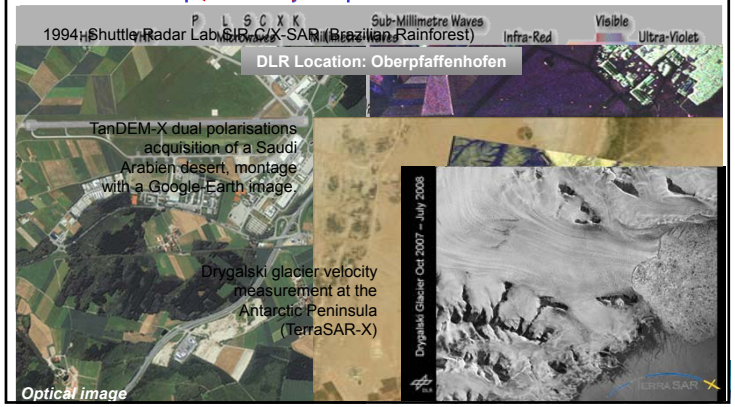

What does the Radar measure ?

Radar reflectivity (backscattered signal) of the target as a function of position.

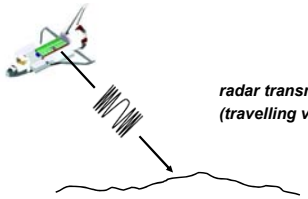

radar transmits a pulse
(travelling velocity is equal to velocity of light)

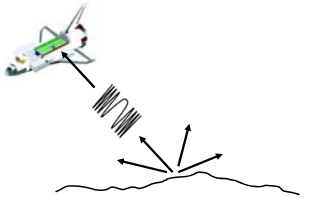

some of the energy in the radar pulse is reflected back towards the radar.

This is what the radar measures.
It is known as radar backscatter σ_o
(sigma nought or sigma zero).

DLR

What does the Radar measure ?

Normalized radar cross-section (backscattering coefficient) is given by:

σ_o *(dB) = 10. Log$_{10}$ (energy ratio)*

whereby

energy ratio = $\frac{\text{received energy by the sensor}}{\text{“energy reflected in an isotropic way”}}$

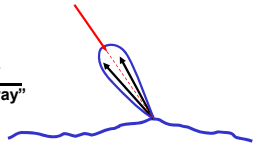

i.e.

The backscattered coefficient can be a positive number if there is a focusing of backscattered energy towards the radar

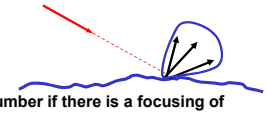

or

The backscattered coefficient can be a negative number if there is a focusing of backscattered energy way from the radar (e.g. smooth surface)

Backscattering Coefficient σ_o

Levels of Radar backscatter	*Typical scenario*
Very high backscatter (above -5 dB)	*man-made objects (urban)* *terrain slopes towards radar* *very rough surface* *radar looking very steep*
High backscatter (-10 dB to 0 dB)	*rough surface* *dense vegetation (forest)*
Moderate backscatter (-20 to -10 dB)	*medium level of vegetation* *agricultural crops* *moderately rough surfaces*
Low backscatter (below -20 dB)	*smooth surface* *calm water* *road* *very dry terrain (sand)*

Commonly Used Frequency Bands

Frequency band	*Frequency range*	*Application examples*
VHF	300 KHz - 300 MHz	foliage/ground penetration, biomass
P-Band	300 MHz - 1 GHz	soil moisture, biomass, penetration
L-Band	1 GHz - 2 GHz	agriculture, forestry, soil moisture
C-Band	4 GHz - 8 GHz	ocean, agriculture
X-Band	8 GHz - 12 GHz	agriculture, ocean, high resolution radar
Ku-Band	14 GHz - 18 GHz	glaciology (snow cover mapping)
Ka-Band	27 GHz - 47 GHz	high resolution radar

Environmental Sensing from Air and Space

Airborne measurements
- Highly flexible operation
- Coverage of dedicated areas
- Experimental configuration
- Sensor specific data formats
- Short re-visit times

Spaceborne measurements
- Highly regular observation
- Wide area coverage
- Highly operational & reliable
- Standard product delivery
- Long term observations


DLR's E-SAR

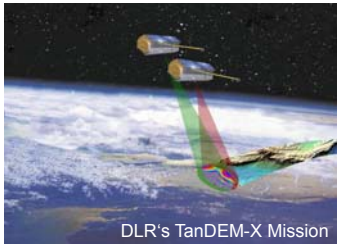
DLR's TanDEM-X Mission

Single Pol (Channel) SAR

Observation Space

Distributed Scatterers:
- Norm. Backscattering Cross Section σ^0;
- Texture (σ^0 statistics).

Deterministic Scatterers:
- Radar Cross Section (RCS);
- Phase of the SAR signal.

Applications

Classification/Segmentation (Texture);
Change detection (Multi temp. analysis);
Glacier velocities (Feature tracking);
Mapping (Feature extraction/Bordering);
Ocean wave/Wind mapping;
Coherent scatterers (CSs).

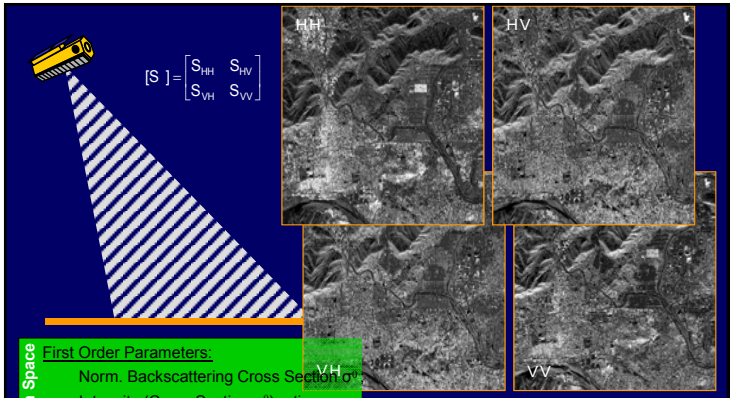

Observation Space

First Order Parameters:
- Norm. Backscattering Cross Section σ^0
- Intensity (Cross Section σ^0) ratios;
- Polarimetric phase differences.

Second Order Parameters:
- Polarimetric (inter channel) coherences

Polarimetric SAR

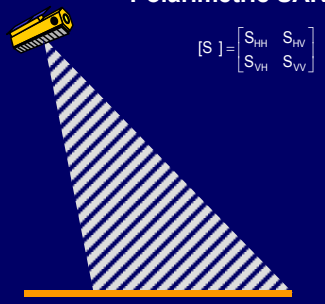

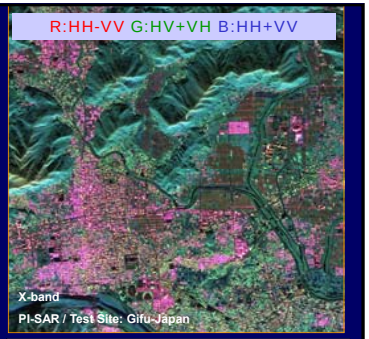

Observation Space

First Order Parameters:
- Norm. Backscattering Cross Section σ^0
- Intensity (Cross Section σ^0) ratios;
- Polarimetric phase differences.

Second Order Parameters:
- Polarimetric (inter channel) coherences

Applications

Soil moisture/roughness estimation;
Wettland/Veg. characterisation/mapping;
Snow & Ice mapping (type classification);
Ship & Oil spill detection;
Classification/Segmentation (Pol based).

The Polarimetric Scattering Problem

Incident (Plane) Wave

$$\vec{E}^{i}_{hv}(\vec{r}) = \begin{bmatrix} E^{i}_{h}(\vec{r}) \\ E^{i}_{v}(\vec{r}) \end{bmatrix}$$

(Jones Vector Representation)

Scattered Field

In the far zone region

$(|\vec{r}| >> \lambda \quad |\vec{r}| >> |\vec{r}'|)$

$$\vec{E}^{s}_{hv}(\vec{r}) = \begin{bmatrix} E^{s}_{h}(\vec{r}) \\ E^{s}_{v}(\vec{r}) \end{bmatrix}$$

(Jones Vector Representation)

Scatterer

Transforms the incident into the scattered wave

2x2 Complex Scattering Matrix

$$\begin{bmatrix} E^{s}_{h}(\vec{r}) \\ E^{s}_{v}(\vec{r}) \end{bmatrix} = \frac{exp(ikr)}{r} \begin{bmatrix} S_{HH}(\vec{r}) & S_{HV}(\vec{r}) \\ S_{VH}(\vec{r}) & S_{VV}(\vec{r}) \end{bmatrix} \begin{bmatrix} E^{i}_{h}(\vec{r}) \\ E^{i}_{v}(\vec{r}) \end{bmatrix}$$

Mapping of the 2-dim incident vector $\vec{E}^{i}_{hv}(\vec{r})$ into the 2-dim scattered vector $\vec{E}^{s}_{hv}(\vec{r})$

The Polarimetric Scattering Problem

Incident (Plane) Wave

$$\vec{E}^{i}_{hv}(\vec{r}) = \begin{bmatrix} E^{i}_{h}(\vec{r}) \\ E^{i}_{v}(\vec{r}) \end{bmatrix}$$

(Jones Vector Representation)

Scattered Field

In the far zone region

$(|\vec{r}| >> \lambda \quad |\vec{r}| >> |\vec{r}'|)$

$$\vec{E}^{s}_{hv}(\vec{r}) = \begin{bmatrix} E^{s}_{h}(\vec{r}) \\ E^{s}_{v}(\vec{r}) \end{bmatrix}$$

(Jones Vector Representation)

Scatterer

Transforms the Incident into the scattered wave

1: Changes the polarisation state of the incident wave

2: Changes the degree of polarisation of the incident wave

2x2 Complex Scattering Matrix

$$\begin{bmatrix} E^{s}_{h}(\vec{r}) \\ E^{s}_{v}(\vec{r}) \end{bmatrix} = \frac{\exp(ikr)}{r} \begin{bmatrix} S_{HH}(\vec{r}) & S_{HV}(\vec{r}) \\ S_{VH}(\vec{r}) & S_{VV}(\vec{r}) \end{bmatrix} \begin{bmatrix} E^{i}_{h}(\vec{r}) \\ E^{i}_{v}(\vec{r}) \end{bmatrix}$$

Mapping of the 2-dim incident vector $\vec{E}^{i}_{hv}(\vec{r})$ into the 2-dim scattered vector $\vec{E}^{s}_{hv}(\vec{r})$

DLR

Slide 13

Coherent Scattering Matrix

… also known as the Jones Matrix in the bistatic and Sinclair Matrix in the monostatic case

$$\begin{bmatrix} E^{s}_{h} \\ E^{s}_{v} \end{bmatrix} = \frac{\exp(ikr)}{r} \begin{bmatrix} S_{HH} & S_{HV} \\ S_{VH} & S_{VV} \end{bmatrix} \begin{bmatrix} E^{i}_{h} \\ E^{i}_{v} \end{bmatrix}$$

Complex Scattering Amplitudes:

S_{IJ} =f(Frequency,Scattering Geometry)

[S] is independent on the polarisation of the incident wave !!!

and depends only on the physical and geometrical properties of the scatterer

Total Scattered Power: $TP = Span\ ([S]) = Trace([S][S]^{+}) = |S_{HH}|^2 + |S_{HV}|^2 + |S_{VH}|^2 + |S_{VV}|^2$

$$[S] = \frac{\exp(ikr)}{r} \begin{bmatrix} |S_{HH}|\exp(i\phi_{HH}) & |S_{HV}|\exp(i\phi_{HV}) \\ |S_{VH}|\exp(i\phi_{VH}) & |S_{VV}|\exp(i\phi_{VV}) \end{bmatrix}$$

$$[S] = \underbrace{\frac{\exp(ikr)\exp(i\phi_{VV})}{r}}_{\text{Absolute Phase Factor}} \underbrace{\begin{bmatrix} |S_{HH}|\exp i(\phi_{HH}-\phi_{VV}) & |S_{HV}|\exp i(\phi_{HV}-\phi_{VV}) \\ |S_{VH}|\exp i(\phi_{VH}-\phi_{VV}) & |S_{VV}| \end{bmatrix}}_{\text{Seven Parameters: 4 Amplitudes \& 3 Phases}}$$

DLR

Slide 14

Bi- & Mono-Static Measurement of the Scattering Matrix

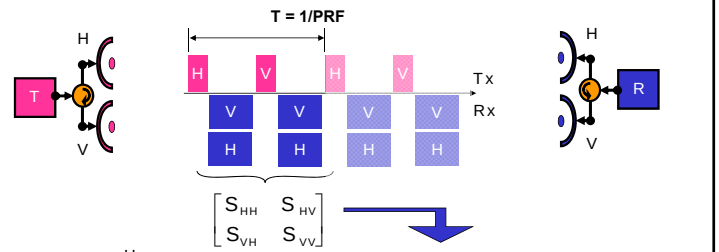

DLR

Slide 15

Scattering Amplitude Images

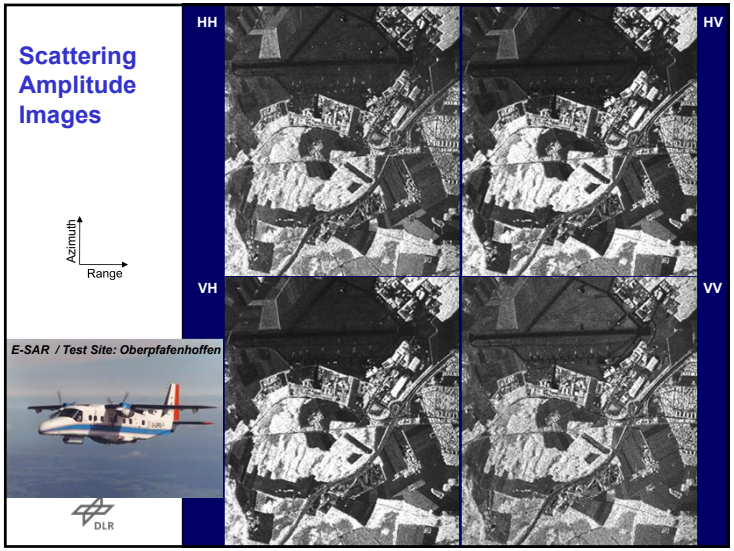

DLR

Backscattering (FSA & BSA)

In the case of monostatic backscattering from reciprocal scatterers:

Reciprocity Theorem $S_{HV}^{BSA} = S_{VH}^{BSA} = S_{XX}^{BSA}$ $(S_{HV}^{FSA} = -S_{VH}^{FSA} = S_{XX}^{FSA})$

$$[S] = \begin{bmatrix} S_{HH} & S_{XX} \\ S_{XX} & S_{VV} \end{bmatrix} \rightarrow [S] = \frac{\exp(i\kappa r)\exp(i\phi_{VV})}{r} \begin{bmatrix} |S_{HH}|\exp i(\phi_{HH}-\phi_{VV}) & |S_{XX}|\exp i(\phi_{XX}-\phi_{VV}) \\ |S_{XX}|\exp i(\phi_{XX}-\phi_{VV}) & |S_{VV}| \end{bmatrix}$$

Absolute Phase Factor — **Five Parameters:** 3 Amplitudes & 2 Phases

The scattering problem can be addressed in the 3-dim complex space:

3-dim Lexicographic (L) and Pauli (P) Scattering Vectors:

$$\vec{k}_{4L} = \begin{bmatrix} S_{HH} \\ S_{XX} \\ S_{XX} \\ S_{VV} \end{bmatrix} \rightarrow \vec{k}_{3L} = \begin{bmatrix} S_{HH} \\ \sqrt{2}S_{XX} \\ S_{VV} \end{bmatrix} \qquad \vec{k}_{4P} = \frac{1}{\sqrt{2}} \begin{bmatrix} S_{HH}+S_{VV} \\ S_{HH}-S_{VV} \\ 2S_{XX} \\ 0 \end{bmatrix} \rightarrow \vec{k}_{3P} = \frac{1}{\sqrt{2}} \begin{bmatrix} S_{HH}+S_{VV} \\ S_{HH}-S_{VV} \\ 2S_{XX} \end{bmatrix}$$

Note: The factor $\sqrt{2}$ is required to keep the vector norm of $\vec{k}_{3L}$ invariant

Partial Scatterers

Deterministic Scatterers

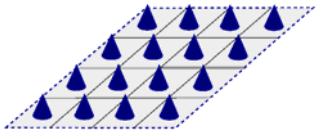

Point Scatterers

- Change the polarisation state of the wave
- Do not change the degree of polarisation

Monochromatic Incident Wave → Monochromatic Scattered Wave

Completely described by [S]

Partial Scatterers

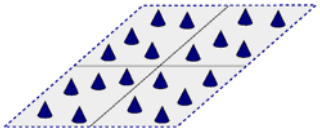

Scatterers with Space or Time Variability

- Change the polarisation state of the wave and also change the degree of polarisation

Depolarisation described by second order statistics

Cannot be described by a single [S]

Covariance & Coherency Matrices in Backscattering

Lexicographic Scattering Vector: → **Covariance Matrix [C]:**

$$\vec{k}_{4L} = [S_{HH} \quad \sqrt{2}S_{XX} \quad S_{VV}]^T$$

$$[C_3] := \begin{bmatrix} \langle|S_{HH}|^2\rangle & \sqrt{2}\langle S_{HH}S_{HV}^*\rangle & \langle S_{HH}S_{VV}^*\rangle \\ \sqrt{2}\langle S_{HV}S_{HH}^*\rangle & 2\langle|S_{HV}|^2\rangle & \sqrt{2}\langle S_{HV}S_{VV}^*\rangle \\ \langle S_{VV}S_{HH}^*\rangle & \sqrt{2}\langle S_{VV}S_{HV}^*\rangle & \langle|S_{VV}|^2\rangle \end{bmatrix}$$

$$[C_3] := \langle \vec{k}_{3L} \cdot \vec{k}_{3L}^{+} \rangle$$

Pauli Scattering Vector: → **Coherency Matrix [T]:**

$$\vec{k}_{3P} = \frac{1}{\sqrt{2}}[S_{HH}+S_{VV} \quad S_{HH}-S_{VV} \quad 2S_{XX}]^T$$

$$[T_3] := \begin{bmatrix} \langle|(S_{HH}+S_{VV})|^2\rangle & \langle(S_{HH}+S_{VV})(S_{HH}-S_{VV})^*\rangle & 2\langle(S_{HH}+S_{VV})S_{HV}^*\rangle \\ \langle(S_{HH}-S_{VV})(S_{HH}+S_{VV})^*\rangle & \langle|(S_{HH}-S_{VV})|^2\rangle & 2\langle(S_{HH}-S_{VV})S_{HV}^*\rangle \\ 2\langle S_{HV}(S_{HH}+S_{VV})^*\rangle & 2\langle S_{HV}(S_{HH}-S_{VV})^*\rangle & 4\langle|S_{HV}|^2\rangle \end{bmatrix}$$

$$[T_3] := \langle \vec{k}_{3P} \cdot \vec{k}_{3P}^{+} \rangle$$

$[C_3]$ and $[T_3]$ are by definition 3x3 hermitian positive semi-definite matrices & contain in general 9 independent parameters

Scattering Polarimetry

INTERPRETATION OF SCATTERING MECHANISMS

- Directly from the Scattering Matrix
- Model based

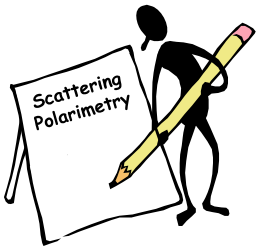

Interpretation of Scattering Mechanisms

Scattering Matrix:

$$[S]=\begin{bmatrix} S_{HH} & S_{HV} \\ S_{HV} & S_{VV} \end{bmatrix}$$

Scattering Vector:

$$\vec{k}_P=\frac{1}{\sqrt{2}}\left[S_{HH}+S_{VV} \quad S_{HH}-S_{VV} \quad 2S_{xx}\right]^T$$

Unitary Representation: $\vec{e}=\frac{1}{|\vec{k}_P|}\vec{k}_P$

$$\vec{e}=\frac{1}{|\vec{k}_P|}\vec{k}_P=\begin{bmatrix} \cos\alpha\exp(i\phi_1) \\ \sin\alpha\cos\beta\exp(i\phi_2) \\ \sin\alpha\sin\beta\exp(i\phi_3) \end{bmatrix}=\frac{1}{\sqrt{2}|\vec{k}_P|}\begin{bmatrix} S_{HH}+S_{VV} \\ S_{HH}-S_{VV} \\ 2S_{XX} \end{bmatrix}$$

Parameterisation of $\vec{e}$ in terms of five angles: $\alpha,\ \beta,\ \phi_1,\ \phi_2,\ \phi_3$

Interpretation of Scattering Mechanisms

Point Reduction Theorem:

$$\vec{e}=\begin{bmatrix} \exp(i\phi_1) & 0 & 0 \\ 0 & \exp(i\phi_2) & 0 \\ 0 & 0 & \exp(i\phi_3) \end{bmatrix}\begin{bmatrix} 1 & 0 & 0 \\ 0 & \cos\beta & -\sin\beta \\ 0 & \sin\beta & \cos\beta \end{bmatrix}\begin{bmatrix} \cos\alpha & -\sin\alpha & 0 \\ \sin\alpha & \cos\alpha & 0 \\ 0 & 0 & 1 \end{bmatrix}\begin{bmatrix} 1 \\ 0 \\ 0 \end{bmatrix}$$

phase — orientation — characteristic

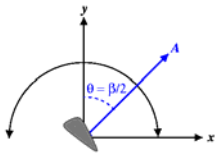

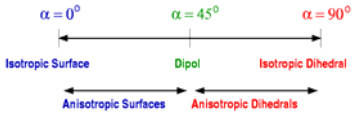

Change of Scattering Mechanism:

$$\vec{e}'=\begin{bmatrix} 1 & 0 & 0 \\ 0 & \cos\Delta\beta & -\sin\Delta\beta \\ 0 & \sin\Delta\beta & \cos\Delta\beta \end{bmatrix}\vec{e} \qquad \vec{e}'=\begin{bmatrix} \cos\Delta\alpha & -\sin\Delta\alpha & 0 \\ \sin\Delta\alpha & \cos\Delta\alpha & 0 \\ 0 & 0 & 1 \end{bmatrix}\vec{e}$$

Interpretation of Scattering Mechanisms

$$\vec{e}'=\begin{bmatrix} 1 & 0 & 0 \\ 0 & \cos\beta & -\sin\beta \\ 0 & \sin\beta & \cos\beta \end{bmatrix}\begin{bmatrix} \cos\alpha & -\sin\alpha & 0 \\ \sin\alpha & \cos\alpha & 0 \\ 0 & 0 & 1 \end{bmatrix}\begin{bmatrix} 1 \\ 0 \\ 0 \end{bmatrix} \quad \text{where} \quad \vec{e}=\begin{bmatrix} 1 \\ 0 \\ 0 \end{bmatrix}=\frac{1}{\sqrt{2}|\vec{k}_P|}\begin{bmatrix} S_{HH}+S_{VV} \\ S_{HH}-S_{VV} \\ 2S_{HV} \end{bmatrix}$$

α=90° and β=0°
Dihedral Scatterer

$$\vec{e}'=\begin{bmatrix} 1 & 0 & 0 \\ 0 & 1 & 0 \\ 0 & 0 & 1 \end{bmatrix}\begin{bmatrix} 0 & 1 & 0 \\ 1 & 0 & 0 \\ 0 & 0 & 1 \end{bmatrix}\begin{bmatrix} 1 \\ 0 \\ 0 \end{bmatrix}=\begin{bmatrix} 0 \\ 1 \\ 0 \end{bmatrix}$$

α=45° and β=0°
H-Dipol Scatterer

$$\vec{e}'=\begin{bmatrix} 1 & 0 & 0 \\ 0 & 1 & 0 \\ 0 & 0 & 1 \end{bmatrix}\begin{bmatrix} 1/\sqrt{2} & 1/\sqrt{2} & 0 \\ 1/\sqrt{2} & 1/\sqrt{2} & 0 \\ 0 & 0 & 1 \end{bmatrix}\begin{bmatrix} 1 \\ 0 \\ 0 \end{bmatrix}=\begin{bmatrix} 1/\sqrt{2} \\ 1/\sqrt{2} \\ 0 \end{bmatrix}$$

α=45° and β=180°
V-Dipol Scatterer

$$\vec{e}'=\begin{bmatrix} 1 & 0 & 0 \\ 0 & -1 & 0 \\ 0 & 0 & -1 \end{bmatrix}\begin{bmatrix} 1/\sqrt{2} & 1/\sqrt{2} & 0 \\ 1/\sqrt{2} & 1/\sqrt{2} & 0 \\ 0 & 0 & 1 \end{bmatrix}\begin{bmatrix} 1 \\ 0 \\ 0 \end{bmatrix}=\begin{bmatrix} 1/\sqrt{2} \\ -1/\sqrt{2} \\ 0 \end{bmatrix}$$

Scattering Processes: Fresnel Scattering

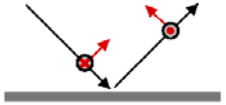

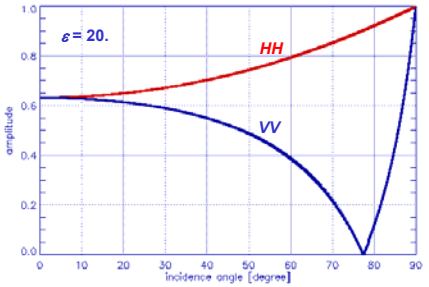

Scattering Matrix: $[S]=\begin{bmatrix} R_H & 0 \\ 0 & R_V \end{bmatrix}$

Fresnel Reflection Coefficients:

$$R_H=\frac{\cos\theta-\sqrt{\varepsilon-\sin^2\theta}}{\cos\theta+\sqrt{\varepsilon-\sin^2\theta}} \quad \text{and} \quad R_V=\frac{\varepsilon\cos\theta-\sqrt{\varepsilon-\sin^2\theta}}{\varepsilon\cos\theta+\sqrt{\varepsilon-\sin^2\theta}}$$

… where e is the dielectric constant of the surface

Scattering Processes: Bragg Scattering

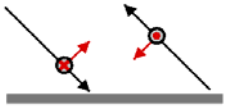

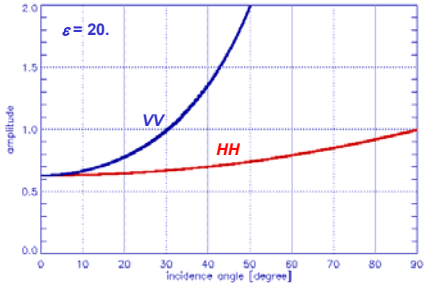

Scattering Matrix: $[S] = \begin{bmatrix} R_H & 0 \\ 0 & R_V \end{bmatrix}$

Bragg Scattering Coefficients:

$$R_H = \frac{\cos\theta - \sqrt{\varepsilon - \sin^2\theta}}{\cos\theta + \sqrt{\varepsilon - \sin^2\theta}} \quad \text{and} \quad R_V = \frac{(\varepsilon - 1)[\sin^2\theta - \varepsilon(1 + \sin^2\theta)]}{\varepsilon\cos\theta + \sqrt{\varepsilon - \sin^2\theta}}$$

… where ε is the dielectric constant of the surface

Scattering Processes: Dihedral Scattering

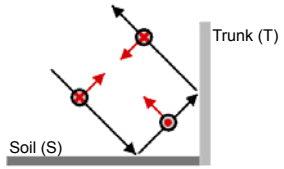

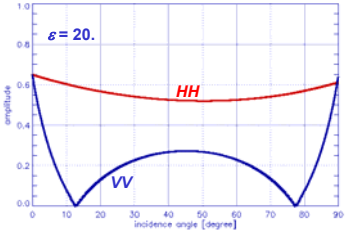

Scattering Matrix:

$$[S] = \begin{bmatrix} 1 & 0 \\ 0 & -1 \end{bmatrix} \begin{bmatrix} 1 & 0 \\ 0 & e^{i\phi} \end{bmatrix} \begin{bmatrix} R_{HS} & 0 \\ 0 & R_{VS} \end{bmatrix} \begin{bmatrix} R_{HT} & 0 \\ 0 & R_{VT} \end{bmatrix} = \begin{bmatrix} R_{HS}R_{HT} & 0 \\ 0 & -R_{VS}R_{VT}e^{i\phi} \end{bmatrix}$$

Fresnel Coefficients:

$$R_{HS} = \frac{\cos\theta - \sqrt{\varepsilon_S - \sin^2\theta}}{\cos\theta + \sqrt{\varepsilon_S - \sin^2\theta}} \quad \text{and} \quad R_{VS} = \frac{\varepsilon_S\cos\theta - \sqrt{\varepsilon_S - \sin^2\theta}}{\varepsilon_S\cos\theta + \sqrt{\varepsilon_S - \sin^2\theta}}$$

$$R_{HT} = \frac{\cos(90-\theta) - \sqrt{\varepsilon_T - \sin^2(90-\theta)}}{\cos(90-\theta) + \sqrt{\varepsilon_T - \sin^2(90-\theta)}} \quad \text{and} \quad R_{VT} = \frac{\varepsilon_S\cos(90-\theta) - \sqrt{\varepsilon_S - \sin^2(90-\theta)}}{\varepsilon_S\cos(90-\theta) + \sqrt{\varepsilon_S - \sin^2(90-\theta)}}$$

Dihedral vs Volume Scattering (L- /P-Band E-SAR – Kryklan/Sweden)

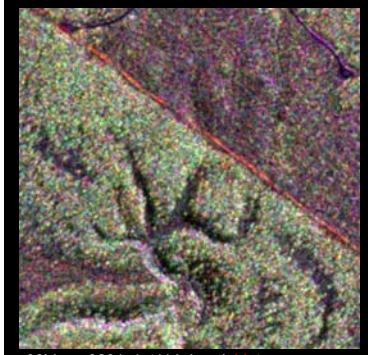

08biosar0201x1_t11 L-band, hh hv vv

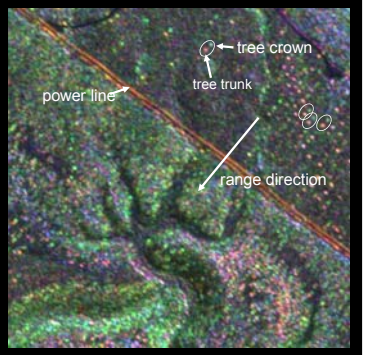

08biosar0302x1_t12 P-band, hh hv vv

Scattering Processes: Volume Scattering

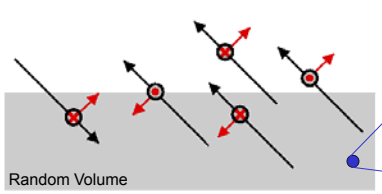

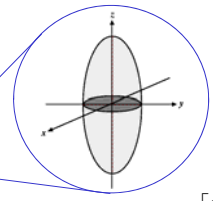

$$\bar{k}(\alpha,\beta,\gamma) = [R_3(\alpha)]\,[R_2(\beta)]\,[R_3(\gamma)]\,\bar{k} \qquad [S] = \begin{bmatrix} a & b \\ b & d \end{bmatrix} \rightarrow \bar{k} = \frac{1}{\sqrt{2}}\begin{bmatrix} a+b \\ a-b \\ 2c \end{bmatrix}$$

Coherency Matrix: $[T] = \left\langle \bar{k}(\alpha,\beta,\gamma)\cdot\bar{k}^{+}(\alpha,\beta,\gamma) \right\rangle$

- $0 \le \alpha \le 2\pi$ Rotation about x-axis
- $0 \le \beta \le \pi$ Rotation about y-axis
- $0 \le \gamma \le 2\pi$ Rotation about z-axis

$$[R_3(\alpha)] = \begin{bmatrix} \cos\alpha & \sin\alpha & 0 \\ -\sin\alpha & \cos\alpha & 0 \\ 0 & 0 & 1 \end{bmatrix} \quad [R_2(\beta)] = \begin{bmatrix} \cos\beta & 0 & -\sin\beta \\ 0 & 1 & 0 \\ \sin\beta & 0 & \cos\beta \end{bmatrix} \quad [R_3(\gamma)] = \begin{bmatrix} \cos\gamma & \sin\gamma & 0 \\ -\sin\gamma & \cos\gamma & 0 \\ 0 & 0 & 1 \end{bmatrix}$$

Scattering Processes: Volume Scattering

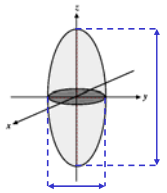

Principal Polarisability Matrix:

$$[P]=\begin{bmatrix}\rho_x & 0 & 0\\ 0 & \rho_y & 0\\ 0 & 0 & \rho_z\end{bmatrix} \quad \text{with} \quad \rho_i=\frac{V}{4\pi(L_i+1/(\varepsilon_r-1))}$$

where $V=\frac{3}{4}\pi\frac{l_x}{2}\frac{l_y}{2}\frac{l_z}{2}$ is the particle volume and

$$L_i=\int_0^\infty \frac{(l_x\,l_y\,l_z)/8}{2(s+l_x/2)^{3/2}(s+l_y/2)^{3/2}(s+l_z/2)^{3/2}}ds \qquad L_x:L_y:L_z=\frac{1}{l_x}:\frac{1}{l_y}:\frac{1}{l_z} \qquad L_x+L_y+L_z=1$$

Particle Anisotropy:

$$A_P:=\frac{L_x(\varepsilon_r-1)+1}{L_y(\varepsilon_r-1)+1}=\frac{m\varepsilon_r+2}{m+\varepsilon_r+1}$$

Particle Shape Ratio:

$$m:=\frac{L_x}{L_y}=\frac{l_y}{l_x} \qquad 0\le m\le\infty$$

$m>1$ oblate spheroids

$m<1$ prolate spheroids

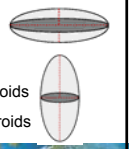

Scattering Processes: Volume Scattering

$$[P](\alpha,\beta,\gamma)=[R_3(\alpha)]\,[R_3(\beta)]\,[R_3(\gamma)]\,[P]\,[R_3(\gamma)]^T[R_3(\beta)]^T[R_3(\alpha)]^T$$

Coherency Matrix:

$$[T]=\int_\alpha\int_\beta\int_\gamma [P](\alpha,\beta,\gamma)\;p(\alpha)\;p(\beta)\;p(\gamma)\;d\alpha\,d\beta\,d\gamma$$

where $p(\alpha)$, $p(\beta)$, $p(\gamma)$ are the pdf's for the corresponding angle distributions

Special Case: Random Volume

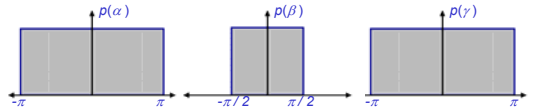

$$[T]=a\begin{bmatrix}1 & 0 & 0\\ 0 & b & 0\\ 0 & 0 & b\end{bmatrix} \quad \text{where} \quad b=\frac{(A_P-1)^2}{2(2+6A_P+7A_P^2)} \qquad 0\le b\le 0.5$$

Scattering Processes: Volume Scattering

Prolate Particles

H/a Loci for varying particle shape and width of distribution

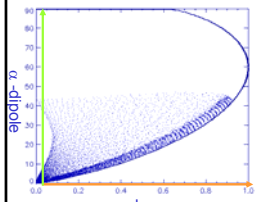

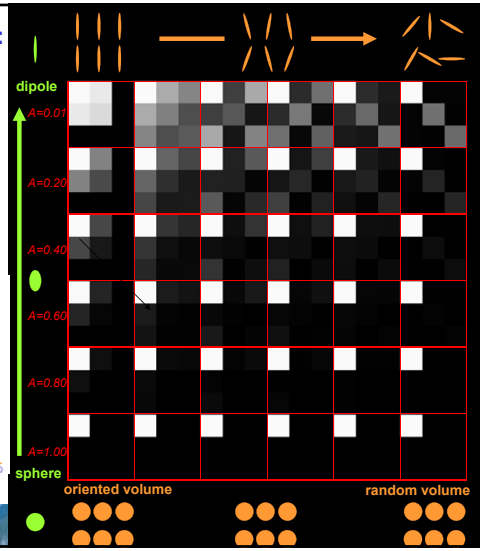

Decomposition Theorems

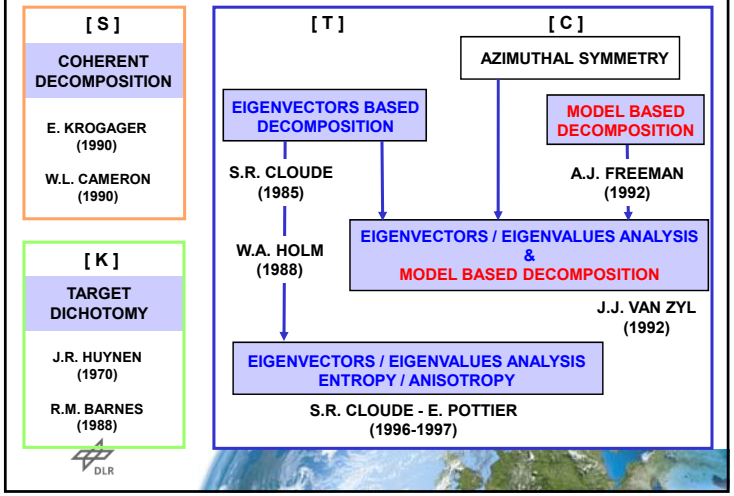

Decomposition Theorems

- **Pauli Matrix Decomp.**
- Model Based Decomp.
- Eigenvector Decomp.

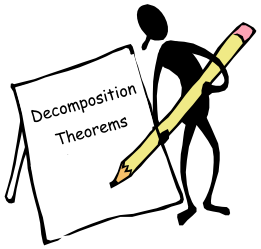

Pauli Matrices Decomposition

$$[S]=\begin{bmatrix} S_{HH} & S_{HV} \\ S_{VH} & S_{VV} \end{bmatrix}=\begin{bmatrix} a+b & c-id \\ c+id & a-b \end{bmatrix}=a\begin{bmatrix} 1 & 0 \\ 0 & 1 \end{bmatrix}+b\begin{bmatrix} 1 & 0 \\ 0 & -1 \end{bmatrix}+c\begin{bmatrix} 0 & 1 \\ 1 & 0 \end{bmatrix}+d\begin{bmatrix} 0 & -i \\ i & 0 \end{bmatrix}$$

- $[S_a]=a\begin{bmatrix} 1 & 0 \\ 0 & 1 \end{bmatrix}$ Single Scattering: $S_{HH}=S_{VV}$
- $[S_b]=b\begin{bmatrix} 1 & 0 \\ 0 & -1 \end{bmatrix}$ Dihedral Scattering: $S_{HH}=-S_{VV}$
- $[S_c]=c\begin{bmatrix} 0 & 1 \\ 1 & 0 \end{bmatrix}$ Dihedral Scattering (… rotated by $\pi/2$ about the LOS)
- $[S_d]=d\begin{bmatrix} 0 & -i \\ i & 0 \end{bmatrix}$ Transforms all polarisation states into their orthogonal states (disappears in backscattering)

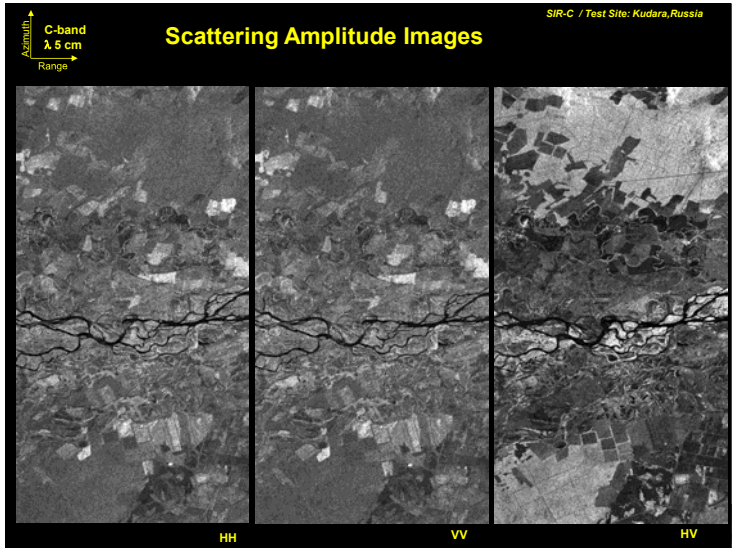

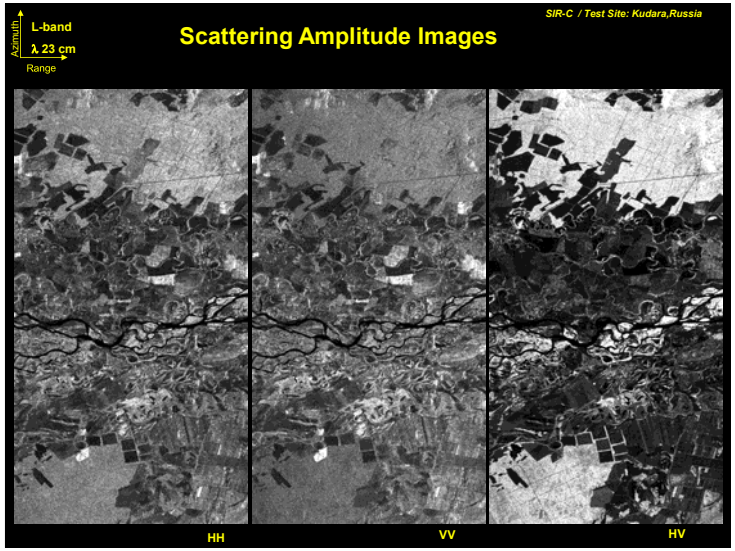

Pauli Images

SIR-C / Test Site: Kudara,Russia

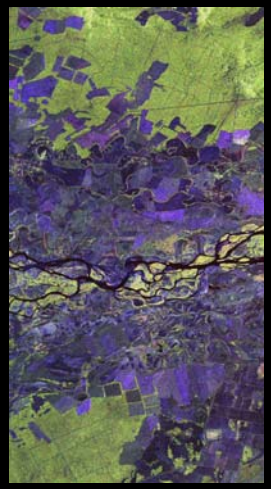

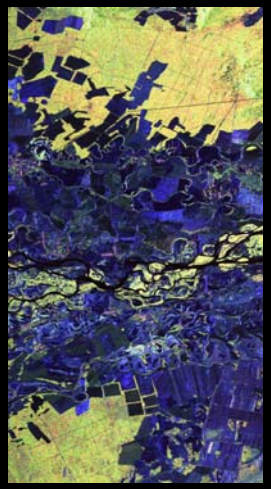

RGB-Coding:
HH-VV
2HV
HH+VV

C-band L-band

Decomposition Theorems

- Pauli Matrice Decomp.
- **Eigenvector Decomp.**
- Model Based Decomp.

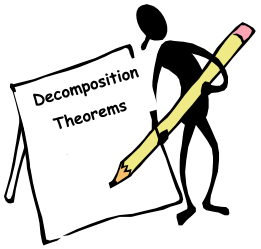

Eigenvector Decomposition

Coherence Matrix: $[T_3] := < \vec{k}_{3P} \cdot \vec{k}_{3P}^{+} >$

Diagonalisation: $[T_3] = [U_3][\Lambda][U_3]^{-1}$

$$[T_3] = \sum_{i=1}^{3} \lambda_i (\vec{e}_i \cdot \vec{e}_i^{+}) = \lambda_1 (\vec{e}_1 \cdot \vec{e}_1^{+}) + \lambda_2 (\vec{e}_2 \cdot \vec{e}_2^{+}) + \lambda_3 (\vec{e}_3 \cdot \vec{e}_3^{+}) = [T_3^1] + [T_3^2] + [T_3^3]$$

$[S_1]$ $[S_2]$ $[S_3]$

- 3 real positive eigenvalues

$$\lambda_1 \geq \lambda_2 \geq \lambda_3 \geq 0$$

- 3 orthonormal eigenvectors

$$\vec{e}_1 = \begin{bmatrix} e_{11} \\ e_{21} \\ e_{31} \end{bmatrix} \quad \vec{e}_2 = \begin{bmatrix} e_{12} \\ e_{22} \\ e_{32} \end{bmatrix} \quad \vec{e}_3 = \begin{bmatrix} e_{13} \\ e_{23} \\ e_{33} \end{bmatrix}$$

where: $[\Lambda] = \begin{bmatrix} \lambda_1 & 0 & 0 \\ 0 & \lambda_2 & 0 \\ 0 & 0 & \lambda_3 \end{bmatrix}$ $[U_3] = \begin{bmatrix} e_{11} & e_{12} & e_{13} \\ e_{21} & e_{22} & e_{23} \\ e_{31} & e_{32} & e_{33} \end{bmatrix}$ $[U_3]^{-1} = [U_3]^{+} = \begin{bmatrix} e_{11}^{*} & e_{21}^{*} & e_{31}^{*} \\ e_{12}^{*} & e_{22}^{*} & e_{32}^{*} \\ e_{13}^{*} & e_{23}^{*} & e_{33}^{*} \end{bmatrix}$

Scattering Entropy / Anisotropy

Coherency Matrix Diagonalisation:

$$[T_3] = \sum_{i=1}^{3} \lambda_i (\vec{e}_i \cdot \vec{e}_i^{+}) = \lambda_1 (\vec{e}_1 \cdot \vec{e}_1^{+}) + \lambda_2 (\vec{e}_2 \cdot \vec{e}_2^{+}) + \lambda_3 (\vec{e}_3 \cdot \vec{e}_3^{+}) = [T_3^1] + [T_3^2] + [T_3^3]$$

Scattering Entropy: $H := \sum_{i=1}^{3} P_i \log_3 P_i$ with: $P_i := \frac{\lambda_i}{\lambda_1 + \lambda_2 + \lambda_3}$

$0 \leq H \leq 1$ where:
- $H = 0$ → Totally Polarised Scatterer
- $H = 1$ → Totally Unpolarised Scatterer

Scattering Anisotropy: $A := \frac{\lambda_2 - \lambda_3}{\lambda_2 + \lambda_3} = \frac{P_2 - P_3}{P_2 + P_3}$

$0 \leq A \leq 1$ where:
- $A = 0$ → 2 Equal Secondary Scattering Processes
- $A = 1$ → Only 1 Secondary Scattering Process

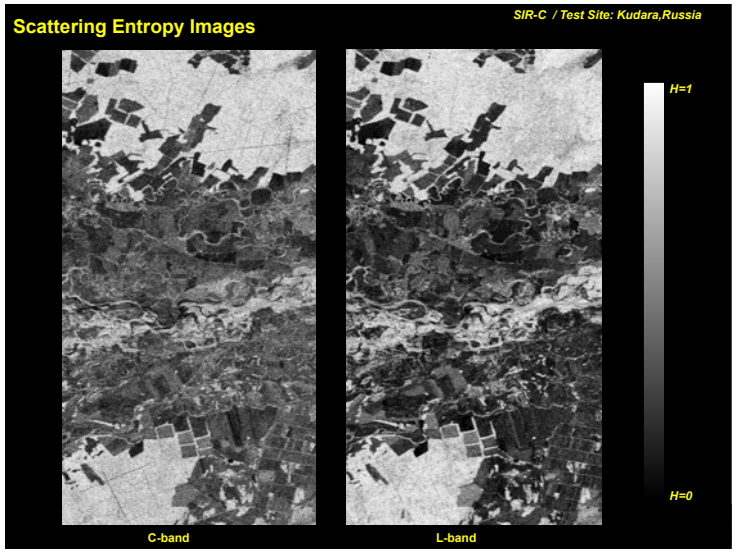

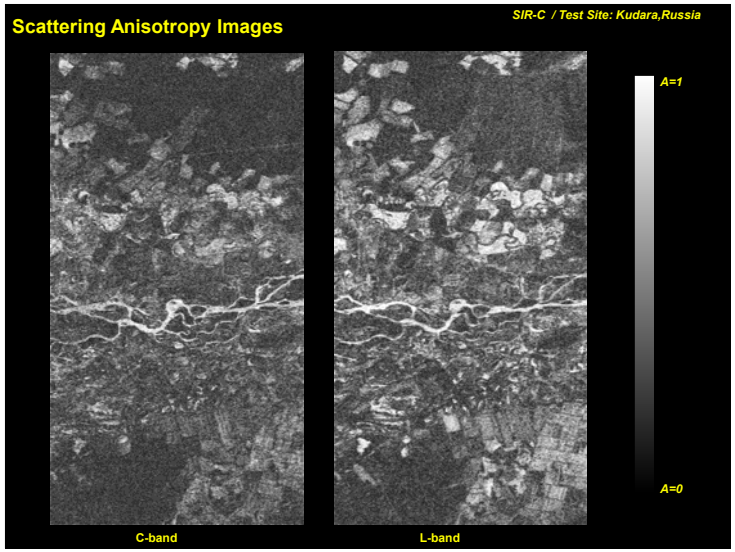

Mean Scattering Parameters: Eigenvector

Coherency Matrix Diagonalisation: $[T_3] = \lambda_1(\vec{e}_1 \cdot \vec{e}_1^{+}) + \lambda_2(\vec{e}_2 \cdot \vec{e}_2^{+}) + \lambda_3(\vec{e}_3 \cdot \vec{e}_3^{+})$

Eigenvectors $\vec{e}_i = \begin{bmatrix} \cos(\alpha_i)\exp(i\gamma_i) \\ \sin(\alpha_i)\cos(\beta_i)\exp(i\delta_i) \\ \sin(\alpha_i)\sin(\beta_i)\exp(i\varepsilon_i) \end{bmatrix}$ Appearance Probabilities: $P_i := \frac{\lambda_i}{\lambda_1 + \lambda_2 + \lambda_3}$

Mean α-Angle: $\alpha = P_1\ \alpha_1 + P_2\ \alpha_2 + P_3\ \alpha_3$

Mean β-Angle: $\beta = P_1\ \beta_1 + P_2\ \beta_2 + P_3\ \beta_3$

Mean γ-Angle: $\gamma = P_1\ \gamma_1 + P_2\ \gamma_2 + P_3\ \gamma_3$

Mean δ-Angle: $\delta = P_1\ \delta_1 + P_2\ \delta_2 + P_3\ \delta_3$

Mean ε-Angle: $\varepsilon = P_1\ \varepsilon_1 + P_2\ \varepsilon_2 + P_3\ \varepsilon_3$

Mean Scattering Mechanism

$\vec{e} = \begin{bmatrix} \cos(\alpha)\exp(i\gamma) \\ \sin(\alpha)\cos(\beta)\exp(i\delta) \\ \sin(\alpha)\sin(\beta)\exp(i\varepsilon) \end{bmatrix}$

DLR

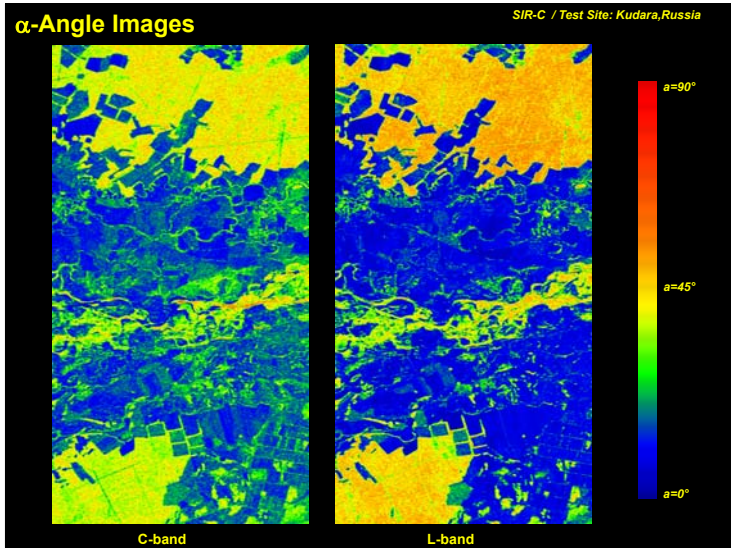

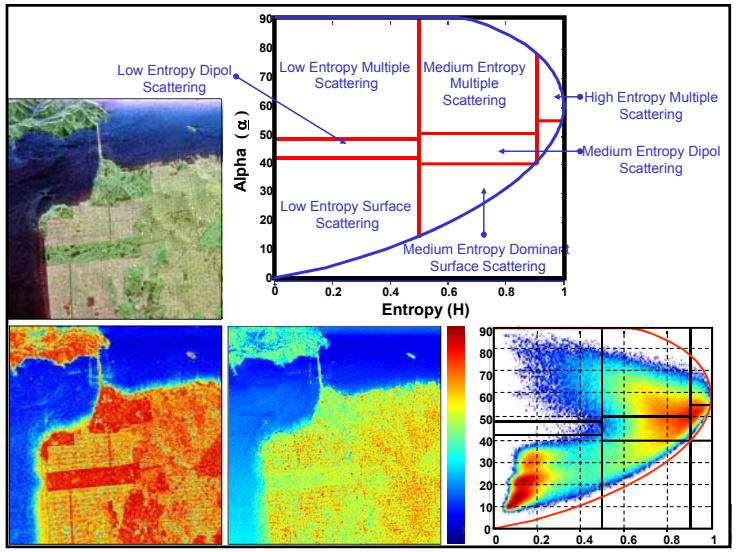

Decomposition Theorems

- Pauli Matrice Decomp.
- Eigenvector Decomp.
- **Model Based Decomp.**

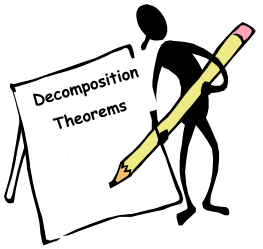

Freeman 3 Component Decomposition

Vegetation Scattering : Bragg-Scattering + Dihedral Scattering + Random Volume of Dipols

$$[T] = [T_S] + [T_D] + [T_V]$$

where $[T_S] = f_S \begin{bmatrix} \beta^2 & \beta & 0 \\ \beta & 1 & 0 \\ 0 & 0 & 0 \end{bmatrix}$ $[T_D] = f_D \begin{bmatrix} \alpha^2 & -\alpha & 0 \\ -\alpha & 1 & 0 \\ 0 & 0 & 0 \end{bmatrix}$ and $[T_V] = f_V \begin{bmatrix} 2 & 0 & 0 \\ 0 & 1 & 0 \\ 0 & 0 & 1 \end{bmatrix}$

$$[T] = \begin{bmatrix} f_S\beta^2 + f_D\alpha^2 + 2f_V & f_S\beta - f_D\alpha & 0 \\ f_S\beta - f_D\alpha & f_S + f_D + f_V & 0 \\ 0 & 0 & f_V \end{bmatrix}$$

4 Equations for 5 Unknowns

- Re(HHVV)-fv/3 > 0 ⟶ Single bounce is dominant ⟶ alpha =1
- Re(HHVV)-fv/3 < 0 ⟶ Double bounce is dominant ⟶ beta =1

3 Component Freeman Decomposition (San Francisco)

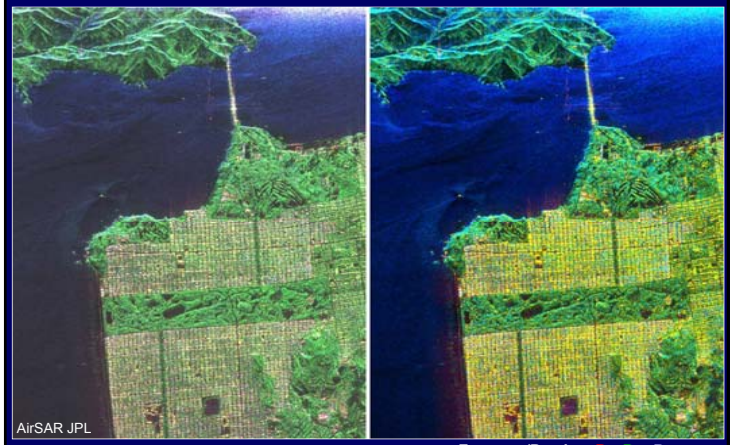

Pauli |HH-VV|, |HV|, HH+VV| Freeman/Durden, P_D, P_V, P_S

Freeman 2 Component Decomposition

$$[T] = [T_{S/D}] + [T_V] \quad \begin{bmatrix} T_{11} & T_{12} & 0 \\ T_{12}^* & T_{22} & 0 \\ 0 & 0 & T_{33} \end{bmatrix} = f_G \begin{bmatrix} |\alpha|^2 & \alpha & 0 \\ \alpha^* & 1 & 0 \\ 0 & 0 & 0 \end{bmatrix} + f_V \begin{bmatrix} 1+\rho & 0 & 0 \\ 0 & 1-\rho & 0 \\ 0 & 0 & 1-\rho \end{bmatrix}$$

Scattering Power Components: $P_G = f_G(1+|\alpha|^2) \qquad P_V = f_V(3-\rho)$

Distinction between dihedral and surface of the ground component:

$|\alpha|<1$ dihedral

$|\alpha|\geq 1$ surface

Volume shape parameter ρ of a randomly oriented volume:

Summary: Polarimetric Parameters / Scattering Matrix

$$[S] = \begin{bmatrix} S_{HH} & S_{XX} \\ S_{XX} & S_{VV} \end{bmatrix} \Rightarrow [S] = \underbrace{\frac{\exp(i\kappa r)\exp(i\varphi_{VV})}{r}}_{\text{Absolute Phase Factor}} \begin{bmatrix} |S_{HH}|\exp i(\varphi_{HH}-\varphi_{VV}) & |S_{XX}|\exp i(\varphi_{XX}-\varphi_{VV}) \\ |S_{XX}|\exp i(\varphi_{XX}-\varphi_{VV}) & |S_{VV}| \end{bmatrix}$$

Five Parameters: 3 Amplitudes & 2 Phases

- **Scattring Amplitudes** $\sigma^0_{HH} := |S_{HH}S^*_{HH}|_N \quad \sigma^0_{XX} := |S_{XX}S^*_{XX}|_N \quad \sigma^0_{VV} := |S_{VV}S^*_{VV}|_N$
- **Total Power** $TP := |S_{VV}|^2 + 4|S_{XX}|^2 + |S_{VV}|^2$
- **Amplitude Ratios** $\sigma^0_{HH}/\sigma^0_{VV} \quad \sigma^0_{XX}/\sigma^0_{VV} \quad \sigma^0_{XX}/(\sigma^0_{HH}+\sigma^0_{VV})$
- **Pol Phase Differences** $\varphi_{HHVV} := \varphi_{HH} - \varphi_{VV}$
- **Helicity** $Hel := |S_{LL}| - |S_{RR}|$

Summary: Second Order Polarimetric Parameters

$$\vec{k}_3 = \begin{bmatrix} A \\ B \\ C \end{bmatrix} \Rightarrow [X_3] := \langle \vec{k}_3 \cdot \vec{k}_3^* \rangle = \begin{bmatrix} \langle AA^* \rangle & \langle AB^* \rangle & \langle AC^* \rangle \\ \langle BA^* \rangle & \langle BB^* \rangle & \langle BC^* \rangle \\ \langle CA^* \rangle & \langle CB^* \rangle & \langle CC^* \rangle \end{bmatrix}$$

Nine Parameters: 3 Real & 3 Complex Elements

Pauli Scat. Vector	Lexico. Scat. Vector
$A := \frac{1}{\sqrt{2}}(S_{HH}+S_{VV})$	$A := S_{HH}$
$B := \frac{1}{\sqrt{2}}(S_{HH}-S_{VV})$	$B := \sqrt{2}S_{XX}$
$C := \sqrt{2}\,S_{XX}$	$C := S_{VV}$

- **Correlation Coefficients** $\gamma_{HHVV} := \frac{|\langle S_{HH}S^*_{VV}\rangle|}{\sqrt{|\langle S_{HH}S^*_{HH}\rangle||\langle S_{VV}S^*_{VV}\rangle|}} \qquad \gamma_{LLRR} := \frac{|\langle S_{LL}S^*_{RR}\rangle|}{\sqrt{|\langle S_{LL}S^*_{LL}\rangle||\langle S_{RR}S^*_{RR}\rangle|}}$
- **Scattering Entropy** $H := \sum_{i=1}^{3} P_i \log_3 P_i \qquad P_i := \frac{\lambda_i}{\lambda_1+\lambda_2+\lambda_3}$
- **Scattering Anisotropy** $A := \frac{\lambda_2-\lambda_3}{\lambda_2+\lambda_3} = \frac{P_2-P_3}{P_2+P_3}$
- **Polarimetric Alpha Angle** $\alpha := P_1\,\alpha_1 + P_2\,\alpha_2 + P_3\,\alpha_3$
- **Polarimetric Beta Angle** $\beta := P_1\,\beta_1 + P_2\,\beta_2 + P_3\,\beta_3$

Applications of Radar Polarimetry

Agriculture/Land-Use

Crop Classification/Moisture Content Estimation
Urban Area mapping
Urban Topography for Mobile comms

Forestry

Biomass Estimation: (Saturates For High Biomass)

C-band saturation at 50 tons/hectare
L-band saturation at 100 tons/hectare
P band saturation at 200 tons/hectare

Deforestation
Forest Canopy Height Estimation
Tree Species Discrimination
Forest Re-growth Monitoring

Geology

Playas :Smooth Natural Surfaces(rms = 1cm)
Alluvial fans, Sand Dunes, Moraines
Sedimentary Rock formations
Lava Flows (extreme in surface roughness)
Weathering Erosion Studies
Surface Roughness Estimates

Hydrology

Flood mapping/Forest Inundation
Snow Hydrology
Soil Moisture

Sea Ice/Oceanography

Ice Roughness/Thickness Studies
Polar Ice Cap Studies
Extra-Terrestrial Ice/Water Studies

Meteorology

Rain rate estimation
Water/Ice particle studies
Severe Storm/Flood warning

Topography/Cartography

Direct Surface Slope Estimation
Accurate DEM Generation
Difference of DEMS for Vegetation mapping

Humanitarian Demining

Surface Penetrating Radar (SPR)
SAR for Mine Field Detection

Soil Moisture Estimation

- Surface characterisation
- mv estimation over bare surface
- mv estimation under the vegetation

Slide 53

Surface Characterisation

VOLUMETRIC MOISTURE CONTENT

m_v [vol. %]

SURFACE ROUGHNESS

rms - height σ [cm]

autocorrelation length l [cm]

The Backscattered signal depends on the moisture, and roughness of the surface.

Single channel SAR cannot resolve unambiguously the bare surface scattering problem.

Slide 54

Models for the Estimation of Bare Surface

Modeling and Inversion

THEORETICAL MODELS

Geometrical-Optic 1963

Physical-Optic 1963

Small Perturbation 1988

Integral Equation 1992

- very complex
- inversion is restricted possible

Shi Model 1997

EMPIRICAL EXTENSIONS

Oh Model 1992

Dubois Model 1995

- inversion with dual pol observables
- based on regressions coefficients of a specific test site

MODEL BASED EXTENSIONS

X-Bragg 1999

- simple model extension
- based on SPM (1st order) with an roughness extension

Time

Slide 56

Models for the Estimation of Vegetated Surface

Modeling and Inversion

THEORETICAL MODELS

Vegetation Models
(Stiles 2000)

- very complex scat. models
- inversion is not possible

SCATTERING DECOMPOSITION APPROACHES

Eigen-Decomposition

Model based-Decomposition

Hajnsek 2009
Jagdhuber 2012

- simple canonical scat. models
- inversion possible

SEMI-MODEL BASED EXTENSIONS

Optimisation
(physical and numerical)

Ari 2010
Neumann 2010

- extended scat. models
- inversion with higher computation time

Time

Slide 57

Small Perturbation Model

$$[S]=\begin{bmatrix} S_{HH} & S_{HV} \\ S_{VH} & S_{VV} \end{bmatrix} = j2k\cos(\theta)Z\begin{bmatrix} R_S(\theta,\ \varepsilon_r) & 0 \\ 0 & R_P(\theta,\ \varepsilon_r) \end{bmatrix}$$ Exact solution of Maxwell Equation for $s \to 0$

$$R_S = \frac{\cos\theta - \sqrt{\varepsilon_r - \sin^2\theta}}{\cos\theta + \sqrt{\varepsilon_r - \sin^2\theta}} \qquad R_P = \frac{(\varepsilon_r - 1)(\sin^2\theta - \varepsilon_r(1+\sin^2\theta))}{(\varepsilon_r\cos\theta + \sqrt{\varepsilon_r - \sin^2\theta})^2}$$

Z = F.T.(E(x, y))

θ = Incidence angle and k = 2π/λ

$\frac{S_{HH}}{S_{VV}} = \frac{R_s}{R_p}$ is independent of roughness

Roughness:

Depolarises the incident wave introducing (depolarised) HV and decreasing polarimetric coherence.

Ambiguity: Terrain Slopes introduce also a HV component but this is co-related to HH and VV.

Polarimetry provides an observation space that allows to separate roughness from moisture effects.

Moisture content:

Effects the scattering amplitude of all polarisations. For "smooth" (with respect to wavelength) surfaces the co-polarimetric ratio (HH/VV) becomes independent of roughness

Small Perturbation Model (Bragg-Model)

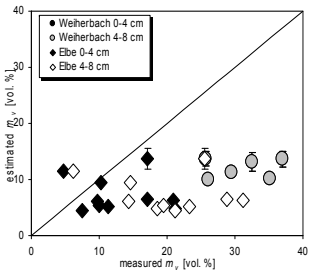

Measured versus estimated volumetric moisture content m_v [vol. %] using SPM

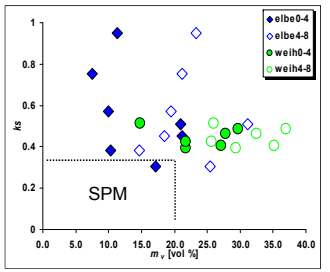

Validity range of the SPM for the ground measurements - surface roughness against volumetric soil moisture

Semi-Empirical Models

Oh-Model

Y. Oh, K. Sarabandi and F.T. Ulaby, "An Empirical Model and an Inversion Technique for Radar Scattering from Bare Soil Surfaces", IEEE Transactions on Geoscience and Remote Sensing, vol. 30, no. 2, pp. 370-381, 1992.

Cross-Pol Amplitude Relation

$$p = \frac{\sigma^0_{hh}}{\sigma^0_{vv}} = \left(1 - \left(\frac{20}{\pi}\right)^{\frac{1}{3|\varepsilon|}} e^{-ks}\right)^2$$

$$q = \frac{\sigma^0_{hv}}{\sigma^0_{vv}} = 0.23\sqrt{\Gamma_0}\left(1 - e^{-ks}\right)$$

s^0_{xx} : backscattering coefficient for different polarisations
q : incidence angle in radians
e_r : real part of the dielectric constant
s : RMS height
k : wavenumber (2p/l)
G_0 : Fresnel reflectivity of the surface at nadir

Dubois-Model

P. C. Dubois, J. J. van Zyl and J. Engman, "Measuring Soil Moisture with Imaging Radar", IEEE Transactions on Geoscience and Remote Sensing, vol. 33, no. 4, pp. 915-926, 1995.

Co-Pol Amplitude Relation

$$\sigma^0_{hh} = 10^{-2.75}\frac{\cos^{1.5}\theta}{\sin\theta^5}10^{0.028\varepsilon\tan\theta}(ks\sin\theta)^{1.4}\lambda^{0.7}$$

$$\sigma^0_{vv} = 10^{-2.35}\frac{\cos^3\theta}{\sin^3\theta}10^{0.046\varepsilon\tan\theta}(ks\sin\theta)^{1.1}\lambda^{0.7}$$

q : incidence angle in radians
e_r : real part of the dielectric constant
s: RMS height
k : wave number (2p/l)
l : wavelength [cm]

Quantitative Estimation of Volumetric Moisture m_v [vol %]

Dubois

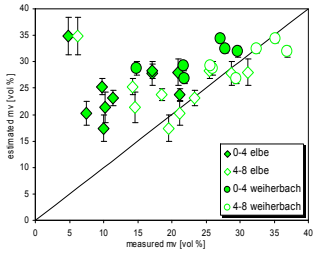

	0-4 cm	4-8 cm	corr.
Elbe RMS_{error}	14	10	-/-
Weih RMS_{error}	11	17	0.2/0.4

Oh

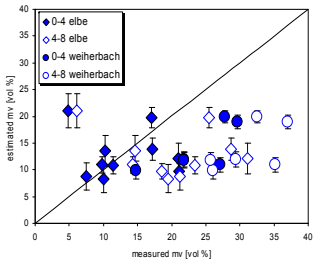

	0-4 cm	4-8 cm	corr.
Elbe RMS_{error}	7	12	-/-
Weih RMS_{error}	18	25	0.5/0.6

Quantitative Estimation of Surface Roughness ks

Dubois

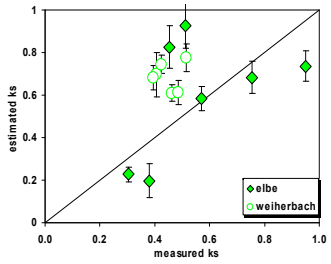

	ks	corr.
Elbe RMS_{error}	0.24	-
Weih RMS_{error}	0.19	-0.7

Oh

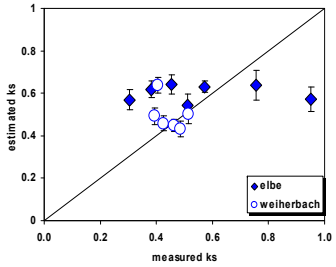

	ks	corr.
Elbe RMS_{error}	0.21	0.6
Weih RMS_{error}	0.19	-0.6

Surface Parameter @ X-Bragg

Surface scattering model for the estimation of soil moisture content & surface roughness

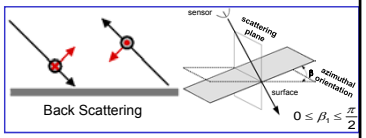

Bragg Surface ⟶ extension ⟶ X-Bragg Surface

$$[T] = \begin{bmatrix} \langle |R_S + R_P|^2 \rangle & \langle (R_S - R_P)(R_S + R_P)^* \rangle & 0 \\ \langle (R_S + R_P)(R_S - R_P)^* \rangle & \langle |R_S - R_P|^2 \rangle & 0 \\ 0 & 0 & 0 \end{bmatrix}$$

Advantage:
- Simple model with direct relation to soil moisture content

Disadvantage:
- not realistic enough for natural surfaces

$$[T] = \begin{bmatrix} C_1 & C_2 \mathrm{sinc}(2\beta_1) & 0 \\ C_2 * \mathrm{sinc}(2\beta_1) & C_3(1+\mathrm{sinc}(4\beta_1)) & 0 \\ 0 & 0 & C_3(1-\mathrm{sinc}(4\beta_1)) \end{bmatrix}$$

Advantage:
- Integration of a roughness & decorrelation term provides natural surface statistics

Disadvantage:
- very sensitive to vegetation cover

$$R_S = \frac{\cos\theta - \sqrt{\varepsilon_r - \sin^2\theta}}{\cos\theta + \sqrt{\varepsilon_r - \sin^2\theta}} \qquad R_P = \frac{(\varepsilon_r - 1)(\sin^2\theta - \varepsilon_r(1+\sin^2\theta))}{(\varepsilon_r \cos\theta + \sqrt{\varepsilon_r - \sin^2\theta})^2} \qquad C_1 = |R_S + R_P|^2 \quad C_2 = (R_S + R_P)(R_S^* - R_P^*) \quad C_3 = \frac{1}{2}|R_S - R_P|^2$$

I. Hajnsek, E. Pottier, S. Cloude, Surface Parameter Estimation using Polarimetric SAR, IEEE TGARS, 2003, vol. 41, no. 4, pp. 727-745

Prediction of the X-Bragg Model I

(HH+VV)(HH-VV) coherence versus b_1 for different local incidence angles

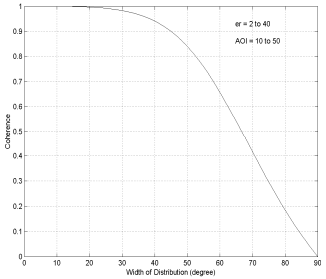

Cross polarised power versus b_1 for different local incidence angles

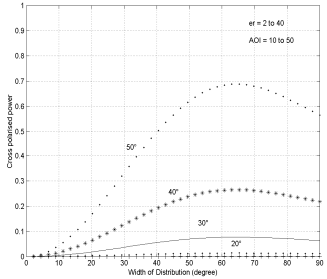

Prediction of the X-Bragg Model II

Variation of Anisotropy with Roughness (Model Parameter β_1)

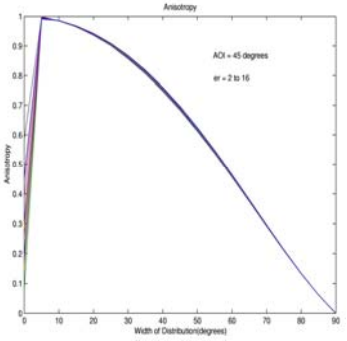

Variation of Entropy/Alpha values with Dielectric Constant (45 degrees AOI)

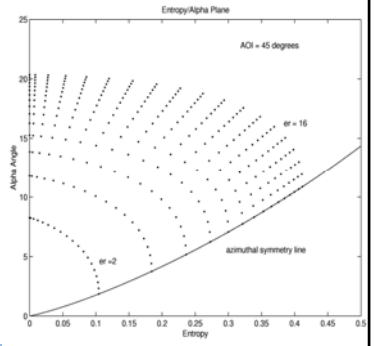

Experimental Data from Anechoic Chamber (JRC - Ispra)

Collected in European Mircowave Signature Laboratory (EMSL)
quad-pol scattering matrix(HH,VV,HV,VH); s = 0.4 cm; surface correlation lenght l = 6;
dielectric constant ε^r = 8; frequency range = 1.5-18.5

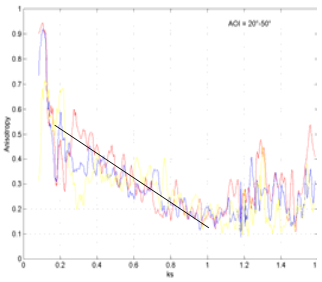

Anisotropy versus frequency plot for the EMSL data

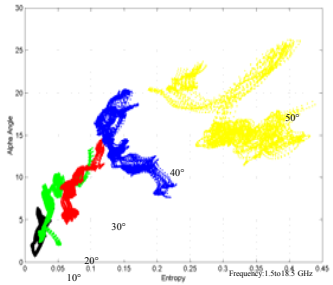

Entropy/alpha angle plot for the EMSL data

Inversion Results @ X-Bragg – Early Example on ELBE 2000

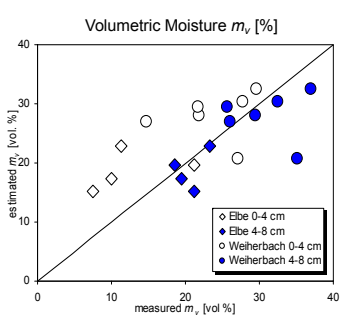

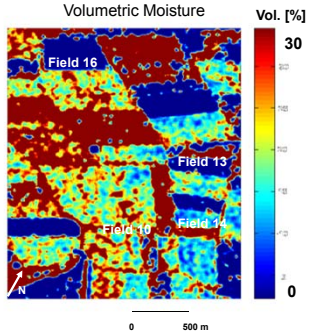

Bare Surfaces: Soil Moisture Estimation @ AQUIFEREX 05

E-SAR / Test Site: Aquiferex, Tunisia

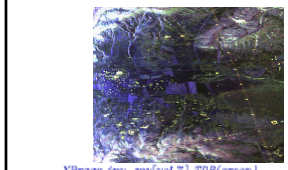

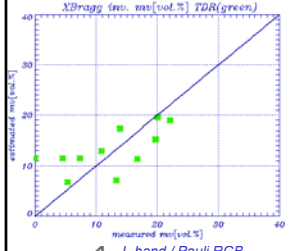

L-band / Pauli RGB

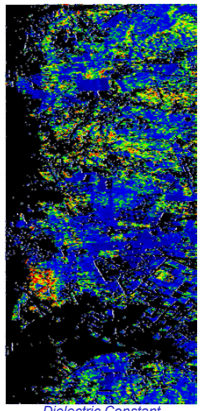

Dielectric Constant

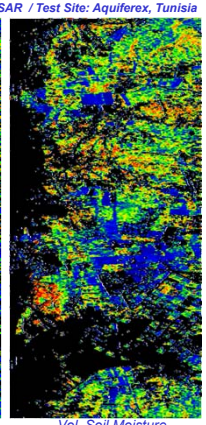

Vol. Soil Moisture

Soil Moisture Estimation

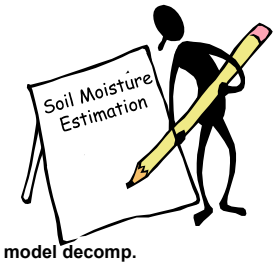

- Surface Characterisation
- mv estimation over bare surface
- **mv estimation under the vegetation**
  - **3 component model decomp.**
  - **improvement of the 3 component model decomp.**
  - **multi-angle approach combined with 3 comp. model decomp.**
  - **hybrid decomposition**

3 Component Freeman Decomposition

$$[T_{Bragg}] = f_S \begin{bmatrix} 1 & \beta^* & 0 \\ \beta & |\beta|^2 & 0 \\ 0 & 0 & 0 \end{bmatrix} \quad \beta = \frac{R_H - R_V}{R_H + R_V}$$

$$R_H = \frac{\cos\theta - \sqrt{\varepsilon_r - \sin^2\theta}}{\cos\theta + \sqrt{\varepsilon_r - \sin^2\theta}}$$

$$R_V = \frac{(\varepsilon_r - 1)(\sin^2\theta - \varepsilon_r(1 + \sin^2\theta))}{(\varepsilon_r \cos\theta + \sqrt{\varepsilon_r - \sin^2\theta})^2}$$

$$f_S \begin{bmatrix} 1 & \beta^* & 0 \\ \beta & |\beta|^2 & 0 \\ 0 & 0 & 0 \end{bmatrix} + f_D \begin{bmatrix} |\alpha|^2 & \alpha & 0 \\ \alpha^* & 1 & 0 \\ 0 & 0 & 0 \end{bmatrix} + \frac{f_V}{4} \begin{bmatrix} 2 & 0 & 0 \\ 0 & 1 & 0 \\ 0 & 0 & 1 \end{bmatrix} = \begin{bmatrix} T_{11} & T_{12} & 0 \\ T_{12}^* & T_{22} & 0 \\ 0 & 0 & T_{33} \end{bmatrix}$$

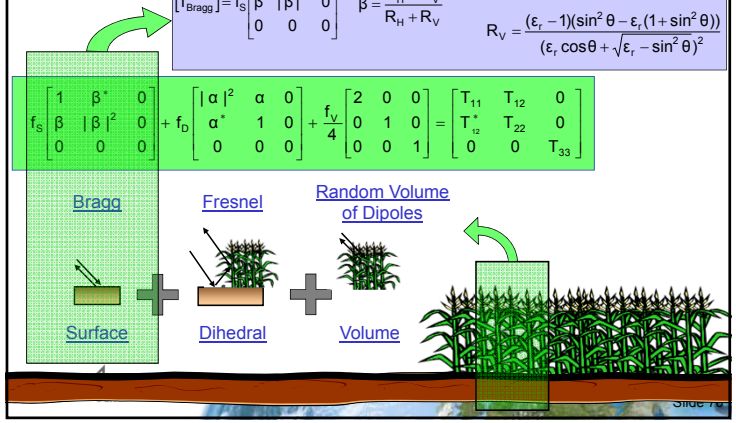

$$[S] = \begin{bmatrix} 1 & 0 \\ 0 & -1 \end{bmatrix} \begin{bmatrix} R_{SS} & 0 \\ 0 & R_{PS} \end{bmatrix} \begin{bmatrix} R_{ST} & 0 \\ 0 & R_{PT} \end{bmatrix} = \begin{bmatrix} R_{SS}R_{ST} & 0 \\ 0 & -R_{PS}R_{PT}e^{i} \end{bmatrix}$$

$$R_{S(S/T)} = \frac{\cos\theta - \sqrt{\varepsilon_{S/T} - \sin^2\theta}}{\cos\theta + \sqrt{\varepsilon_{S/T} - \sin^2\theta}}$$

$$R_{P(S/T)} = \frac{\varepsilon_{S/T}\cos\theta - \sqrt{\varepsilon_{S/T} - \sin^2\theta}}{\varepsilon_{S/T}\cos\theta + \sqrt{\varepsilon_{S/T} - \sin^2\theta}}$$

$$f_S \begin{bmatrix} 1 & \beta^* & 0 \\ \beta & |\beta|^2 & 0 \\ 0 & 0 & 0 \end{bmatrix} + f_D \begin{bmatrix} |\alpha|^2 & \alpha & 0 \\ \alpha^* & 1 & 0 \\ 0 & 0 & 0 \end{bmatrix} + \frac{f_V}{4} \begin{bmatrix} 2 & 0 & 0 \\ 0 & 1 & 0 \\ 0 & 0 & 1 \end{bmatrix} = \begin{bmatrix} T_{11} & T_{12} & 0 \\ T_{12}^* & T_{22} & 0 \\ 0 & 0 & T_{33} \end{bmatrix}$$

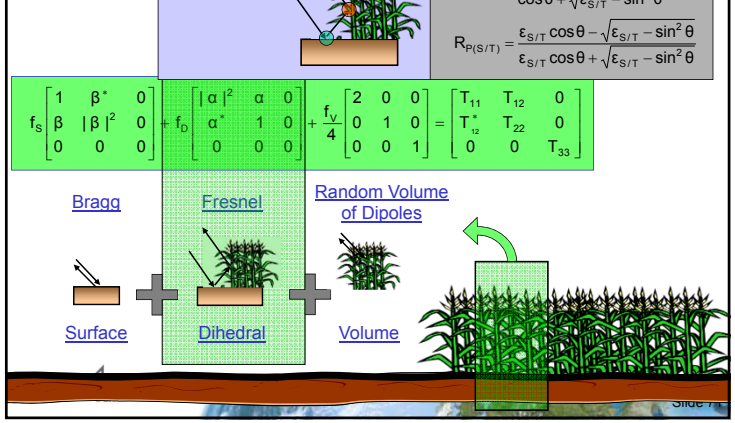

AGRISAR Campaign in Northern Germany 2006

1. Agricultural data base over a whole vegetation growth period - April - August 2006
2. 16 data acquistions (DLR's E-SAR) & ground measurements
3. Support by ESA for the space segment - Sentinel Program

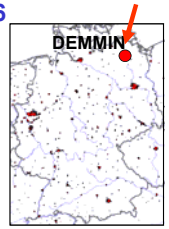

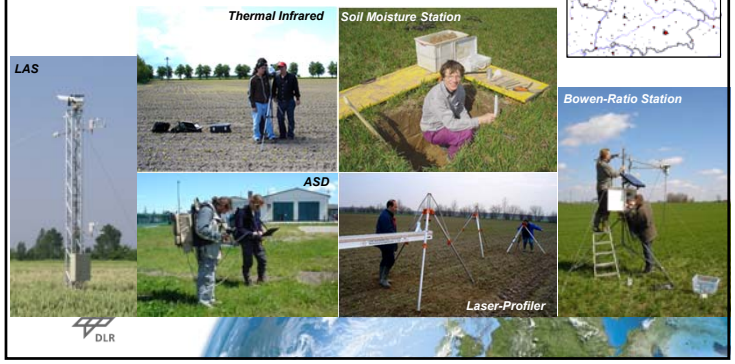

Freeman-Durden 3-Component Decomposition (AGRISAR 2006)

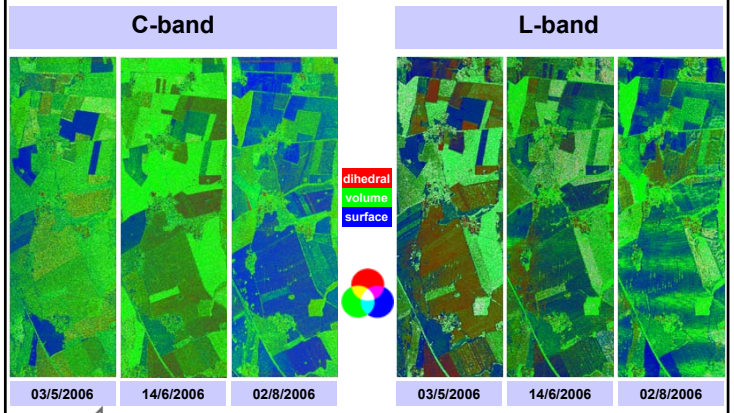

Slide 73

3 Component Decomposition and Modifications

Surface Dihedral Volume

Decision rule $= \begin{matrix} \mathrm{Re}\langle S_{HH} S_{VV}^{*} \rangle > 0 \\ \alpha = 0 \end{matrix}$ or $\begin{matrix} \mathrm{Re}\langle S_{HH} S_{VV}^{*} \rangle < 0 \\ \beta = 0 \end{matrix}$

Surface modification (X-Bragg) (ε_s, θ, δ):

$$[T_{xB}] = f_S \begin{bmatrix} 1 & \beta^{*}\,\mathrm{sinc}(2\delta) & 0 \\ \beta\,\mathrm{sinc}(2\delta) & \frac{1}{2}|\beta|^2 (1+\mathrm{sinc}(4\delta)) & 0 \\ 0 & 0 & \frac{1}{2}|\beta|^2 (1-\mathrm{sinc}(4\delta)) \end{bmatrix}$$

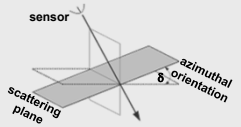

→ Incorporation of a roughness and HV-decorrelation term (δ)

[Hajnsek et al., 2001]

Dihedral modification (modified Fresnel coefficients) (ε_s, ε_i, θ, φ, L_S):

$$[T_{moD}] = f_D \cdot |L_S^2| \cdot \begin{bmatrix} |\alpha|^2 & \alpha & 0 \\ \alpha^{*} & 1 & 0 \\ 0 & 0 & 0 \end{bmatrix} \qquad 0 < L_S \le 1$$

$$L_S = \exp(-2 \cdot (ks)^2 \cdot \cos(\theta)^2) \qquad ks = 1 - A$$

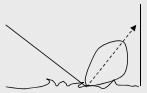

→ Incorporation of a surface scattering loss L_S

[Lee et al., 2005]

[Freeman & Durden, 1998, Yamaguchi et al., 2006]

DLR

Slide 74

Modified Decompositions @ L-band for 03/5/2006

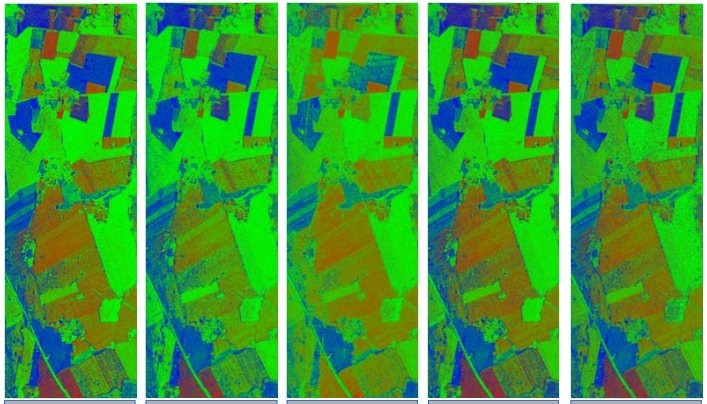

X-Bragg | Modified Dihedral | Volume 1 | Volume 2 | Volume 3

DLR

Slide 75

Time Series of Decompositions on Field Basis @ L-band

Wheat (No. 250) – far range

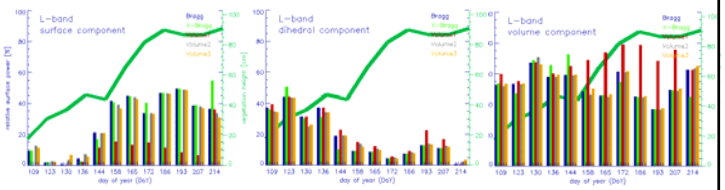

Wheat (No. 230) – near range

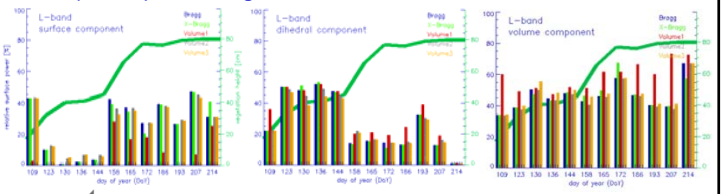

DLR

Slide 76

Time Series of Decompositions on Field Basis @ L-band

Rape (No. 140) – near range

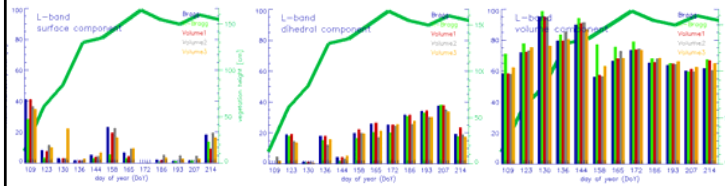

Rape (No. 101) – far range

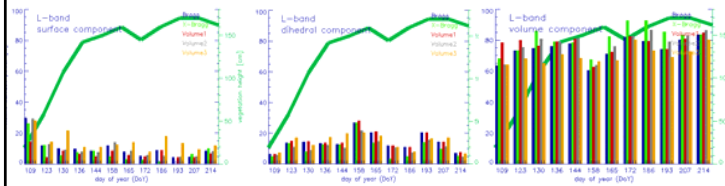

DLR

Slide 77

Inverted Soil Moisture @ L-band Volume 2 (surface) and modified Dihedral (dihedral)

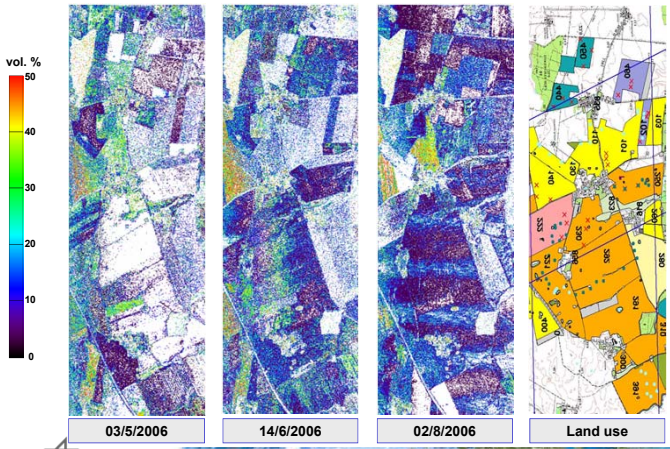

Slide 78

Time Series of Inverted Soil Moisture @ L-band

Wheat field (No. 250) *Wheat field (No. 230)*

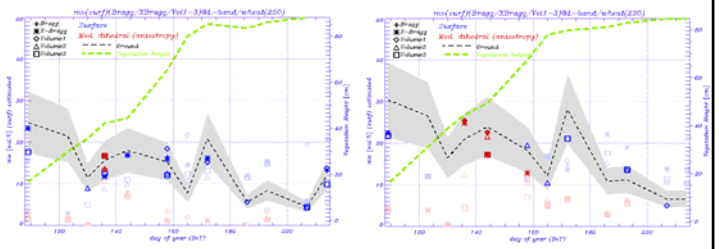

+ Bragg ∗X-Bragg ◇Volume 1 △Volume 2 □Volume 3

Surface Dihedral ±30% Intervall

Slide 79

Time Series of Inverted Soil Moisture @ L-band

Rape field (No. 140) *Rape field (No. 101)*

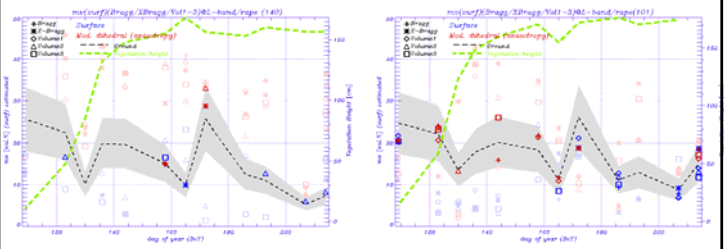

+ Bragg ∗X-Bragg ◇Volume 1 △Volume 2 □Volume 3

Surface Dihedral ±30% Intervall

Slide 80

Soil Moisture Estimation

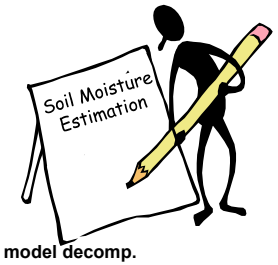

- Surface Characterisation
- mv estimation over bare surface
- **mv estimation under the vegetation**
  - 3 component model decomp.
  - **improvement of the 3 component model decomp.**
  - multi-angle approach combined with 3 comp. model decomp.
  - hybrid decomposition

Slide 81

Polarimetric Decomposition Techniques & Inversion Scheme

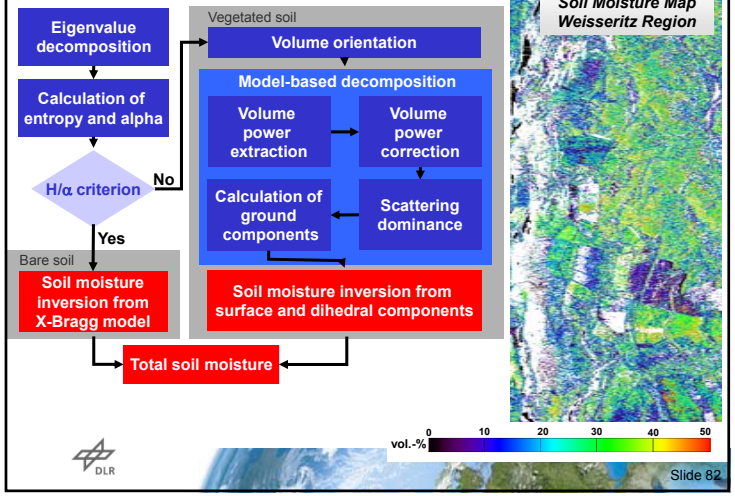

Modeling of Volume Orientation

Volume modelling of a cloud of uniformly ***shaped*** (ρ) particles with an ***orientation*** (τ) in azimuthal direction

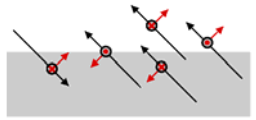

Selection of volume orientation by **polarisation power ratio** P_r:

$$P_r = 10 \cdot \log \frac{\langle |S_{VV}|^2 \rangle}{\langle |S_{HH}|^2 \rangle}$$

General Case	Vertical dipoles [Pr < -2dB]	Random dipoles [-2dB < Pr < 2dB]	Horizontal dipoles [Pr > 2dB]
	$pdf(\tau) = \frac{1}{2} \cdot \sin(\tau)$ $0 < \tau \leq \pi$	$pdf(\tau) = \frac{1}{2\pi}$ $0 < \tau \leq 2\pi$	$pdf(\tau) = \frac{1}{2} \cdot \cos(\tau)$ $-\pi/2 < \tau \leq \pi/2$
$[T_V] = f_V \begin{bmatrix} C1 & C4 & 0 \\ C4 & C2 & 0 \\ 0 & 0 & C3 \end{bmatrix}$	$[T_V] = \frac{f_V}{30} \begin{bmatrix} 15 & 5 & 0 \\ 5 & 7 & 0 \\ 0 & 0 & 8 \end{bmatrix}$	$[T_V] = \frac{f_V}{4} \begin{bmatrix} 2 & 0 & 0 \\ 0 & 1 & 0 \\ 0 & 0 & 1 \end{bmatrix}$	$[T_V] = \frac{f_V}{30} \begin{bmatrix} 15 & -5 & 0 \\ -5 & 7 & 0 \\ 0 & 0 & 8 \end{bmatrix}$

[Yamaguchi et al., 2005]

Correction of Volume Intensity f_v with Eigen-based analysis

$$\begin{bmatrix} T_{11} & T_{12} & 0 \\ T_{12}^* & T_{22} & 0 \\ 0 & 0 & T_{33} \end{bmatrix} - f_v \cdot \begin{bmatrix} C_1 & C_4 & 0 \\ C_4 & C_2 & 0 \\ 0 & 0 & C_3 \end{bmatrix} = [T_{Surface}] + [T_{Dihedral}]$$

Eigenanalysis of Ground Components

Set Eigenvalues to zero (lower calculus limit)

Solutions for fv :

$$f_{v_1} = 4T_{33}$$

$$f_{v_{2,3}} = T_{11} + 2T_{22} \pm \sqrt{T_{11}^2 + 8T_{12} \cdot T_{12}^* - 4T_{11} \cdot T_{22} + 4T_{22}^2}$$

Solution → ***Negative Powers = Too Strong Volume Subtraction!***

Find Minimum → ***Decomposiition with Corrected Volume Intensity fvcorr***

[van Zyl et al., 2008]

3 Component Decomposition and Modifications

Surface Dihedral Volume

Scattering dominance = $\alpha = 0$ $\mathrm{Re}\langle S_{HH} S_{VV}^* \rangle > 0$ or $\beta = 0$ $\mathrm{Re}\langle S_{HH} S_{VV}^* \rangle < 0$

Surface model (X-Bragg) (ε_s, θ, δ):

$$[T_{XB}] = f_S \begin{bmatrix} 1 & \beta^* \mathrm{sinc}(2\delta) & 0 \\ \beta \mathrm{sinc}(2\delta) & \frac{1}{2}|\beta|^2 (1 + \mathrm{sinc}(4\delta)) & 0 \\ 0 & 0 & \frac{1}{2}|\beta|^2 (1 - \mathrm{sinc}(4\delta)) \end{bmatrix}$$

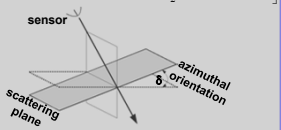

→ Incorporation of a roughness and HV-decorrelation term [Hajnsek et al., 2001]

Dihedral model (Fresnel with vegetation attenuation) (ε_s, ε_b, θ, φ, L_V):

$$[T_{moD}] = f_D \cdot L_V \cdot \begin{bmatrix} |\alpha|^2 & \alpha & 0 \\ \alpha^* & 1 & 0 \\ 0 & 0 & 0 \end{bmatrix}$$

$$L_V = \exp(-1/(\mu_{\max} - \mu_{\min}))$$

$$\mu_{\max} = \frac{\lambda_1}{P_V}$$

$$\mu_{\min} = \frac{\lambda_2}{P_V}$$

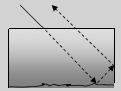

→ Incorporation of a vegetation attenuation L_V

OPAQUE – Campaign

May 2007

1. Soil moisture estimation under different land cover with measurement approaches at different scales
   2 Radar data acquisition flights (single pol X-, dual-pol C- and quad-pol L- and P-band)
   Ground measurements (soil moisture, soil roughness, biomass,…)
2. Goal: Support flood forecasting by identification of critical catchment states

TDR and GPR

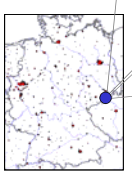

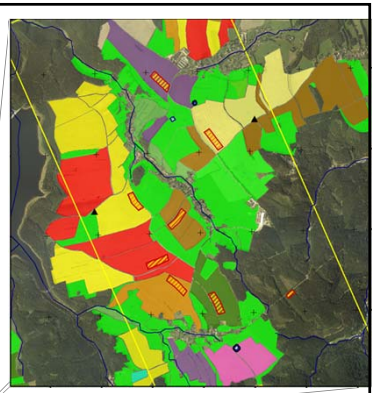

DLR

Slide 87

Volume Orientation and Scattering Dominance @ L-band

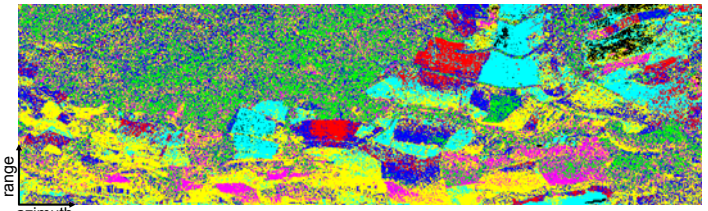

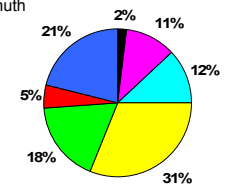

volume orientation	surface dominant	dihedral dominant
vertical		
horizontal		
random		

X-Bragg only

DLR

Slide 88

Model-based Decomposition @ L-band

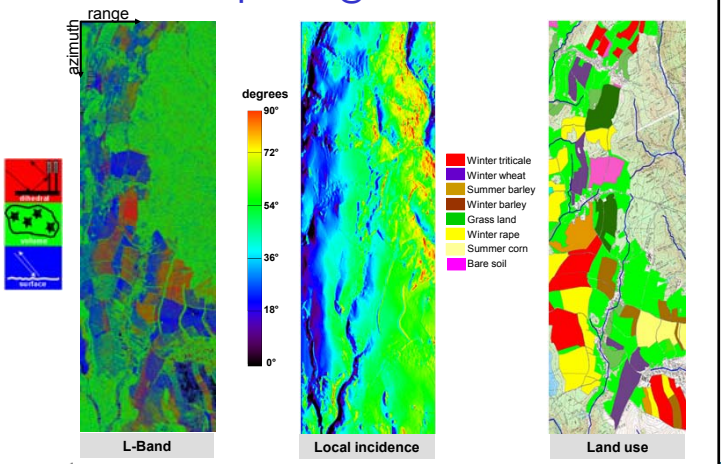

DLR

Slide 89

Inverted Soil Moisture @ L-band

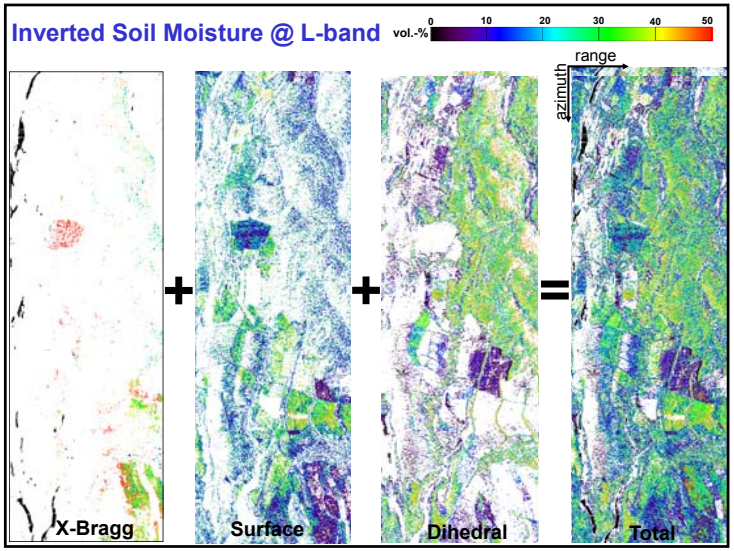

Validation with TDR Measurements on Winter Wheat

Vegetation height:
55cm
Row distance:
10cm
Wet biomass:
2,85kg/m²




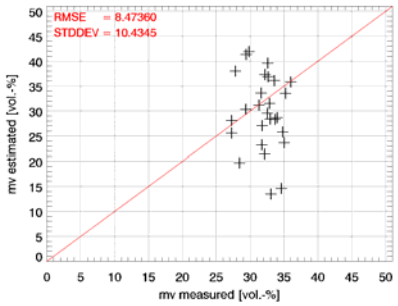

Slide 91

Validation with TDR Measurements on Summer Barley

Vegetation height:
45cm
Row distance:
23cm
Wet biomass:
0,93kg/m²




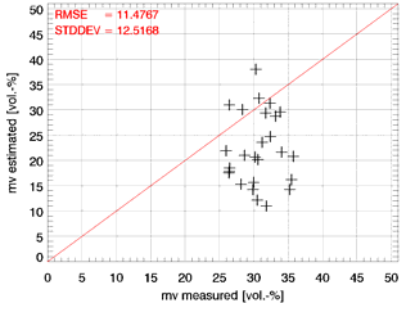

Slide 92

Validation with TDR Measurements on Winter Triticale

Vegetation height:
85cm
Row distance:
10cm
Wet biomass:
3,34kg/m²


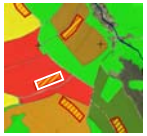

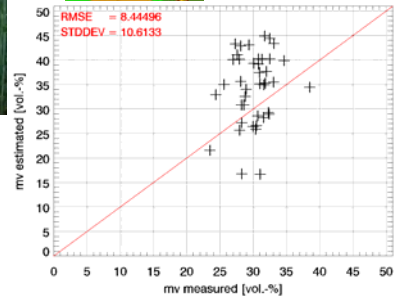

Slide 93

Validation with TDR Measurements on Winter Barley

Vegetation height:
70cm
Row distance:
10cm
Wet biomass:
3,31kg/m²


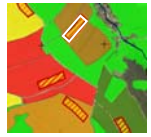

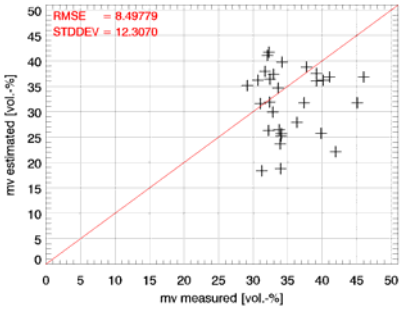

Slide 94

Soil Moisture Estimation

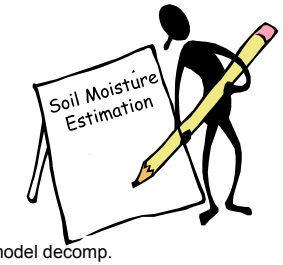

- Surface Characterisation
- mv estimation over bare surface
- **mv estimation under the vegetation**
  - 3 component model decomp.
  - improvement of the 3 component model decomp.
  - **multi-angle approach combined with 3 comp. model decomp.**
  - hybrid decomposition

Multi-Angle Approach for Soil Moisture Inversion Rate Increase

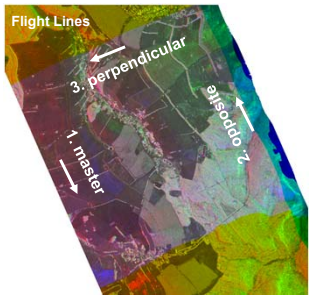

Testsite: Weisseritz Watershed; E-SAR L-band

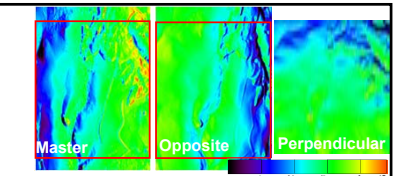

Single angular 1 acquisition	Bi-angular 2 acquisitions	Tri-angular 3 acquisitions
master	master - perpendicular	master - opposite - perpendicular

Inversion Rate of Soil Moisture Estimation @ different AOI

One acquisition	**master**	**opposite**	**perpendicular**
Single angular	40.32%	29.87%	48.53%
Two acquisitions	**master-opposite**	**master-perpendicular**	**opposite-perpendicular**
Bi-angular	55.87%	63.39%	60.71%
Three acquisitions	**master-opposite-perpendicular**		
Tri-angular	70.89%		

Validation of Soil Moistures @ different Incidence Angles

Sampling box: 13x13 pixels
Box coverage: 70%

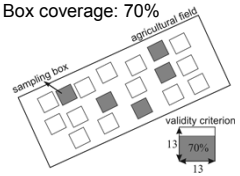

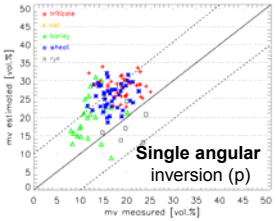

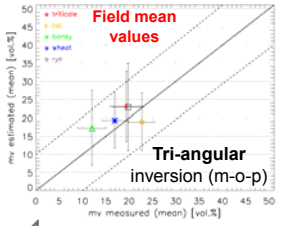

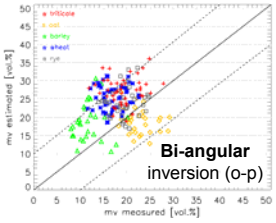

RMSE [vol.%] between Estimated and Measured Soil Moistures for Different Incidence Angle Constellations

Fields	m	o	p	m-o	m-p	o-p	m-o-p
Winter Triticale	6.34	6.34	10.33	5.42	6.27	9.46	5.72
Winter Barley	<	<	9.75	7.76	6.85	8.78	6.94
Winter Rye	5.25	6.11	5.86	5.81	4.89	6.42	5.27
Winter Wheat	4.52	<	9.79	4.41	5.04	9.54	4.98
Summer Oat	8.55	6.43	-	6.35	8.55	6.43	6.35
Mean	6.17	6.29	8.93	5.95	6.32	8.13	5.85
	Single angular			Bi-angular			Tri-angular

- = out of scene
< = too less values for a valid analysis

RMSE @ Different Incidence Angle Constellations

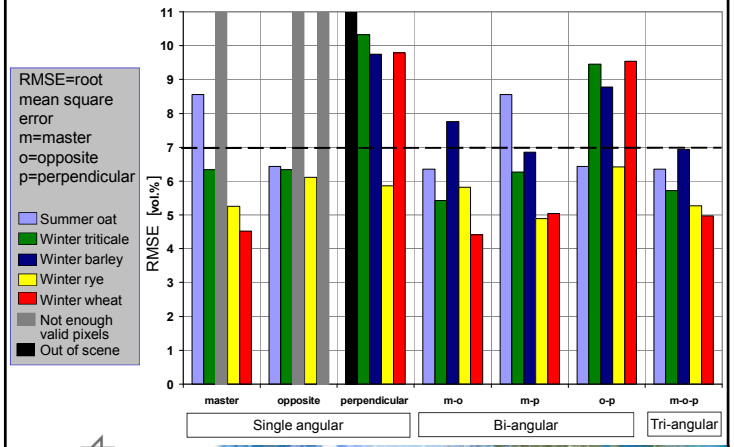

Soil Moisture Estimation

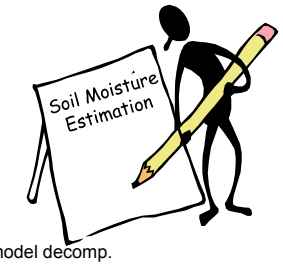

- Surface Characterisation
- mv estimation over bare surface
- **mv estimation under the vegetation**
  - 3 component model decomp.
  - improvement of the 3 component model decomp.
  - multi-angle approach combined with 3 comp. model decomp.
  - **hybrid decomposition**

Basic Principle of Hybrid Polarimetric Decomposition

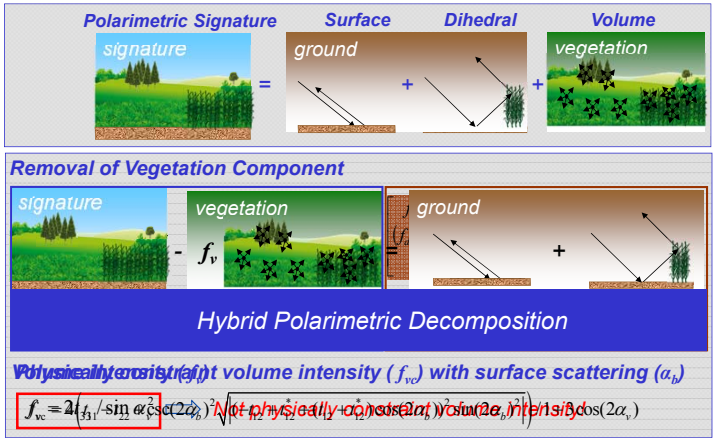

Retrieval of the Ground Scattering Components

signature - vegetation f_{vc} = $\begin{bmatrix} f_s\cos^2\zeta + f_d\sin^2\alpha_d^2 & (f_d - f_s)\cos\alpha_{d,s}\sin\alpha_{d,s} & 0 \\ (f_d - f_s)\cos\alpha_{d,s}\sin\alpha_{d,s} & f_d\cos^2\zeta + f_s\sin^2\alpha_d^2 & 0 \\ 0 & 0 & f_v \end{bmatrix}$

Hybrid Polarimetric Decomposition

Eigen-based Decomposition of Ground Components

- From eigenvalues:
- From eigenvectors: **Intensity** of ground (f_d, f_s)

Physically Meaningful Separation of Scattering Mechanisms (α_d, α_s)

Scattering mechanisms of ground (α_d, α_s)

$\alpha_d + \alpha_s = \pi/2$ Orthogonality condition

- $\alpha \in [0, \pi/4]$ Surface scattering → α_s
- $\alpha \in [\pi/4, \pi/2]$ Dihedral scattering → α_d

103

DLR

Slide 103

Soil Moisture Inversion from Surface Scattering Component

Polarimetric SAR data

Surface scattering component from **hybrid polarimetric decomposition**

$\beta = -\tan(\alpha_s)$

Surface scattering model

Bragg scatter modeling with θ_{loc} and a **variety of soil dielectric constants** ε_S

$\beta_m = \frac{R_{HH} - R_{VV}}{R_{HH} + R_{VV}}$

$R_{HH}, R_{VV} = f(\varepsilon_S, \theta_{loc})$

data

Minimization $\min_{\varepsilon_s}\{|\beta - \beta_m|\}$

model

ε_S

Pedo-Transfer Function of

Topp et al. (ε_S<40)

Roth et al. (ε_S>40)

Soil moisture [vol.%]

DLR

Slide 104

Soil Moisture Inversion along Vegetation Growth Cycle

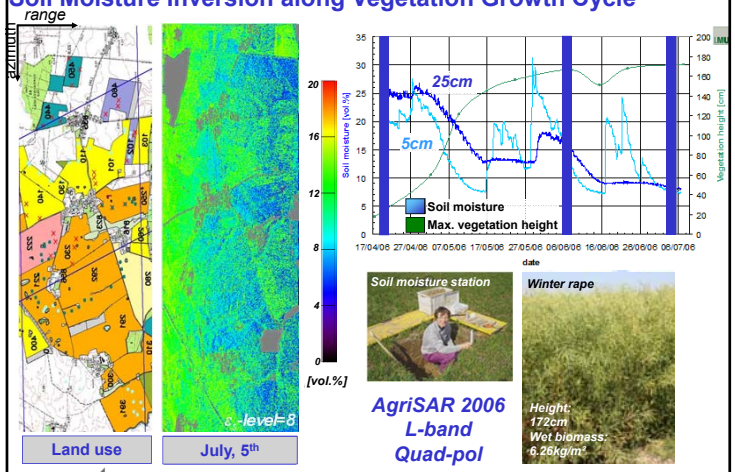

DLR

Validation of Moisture Inversion with Field Measurements (TDR)

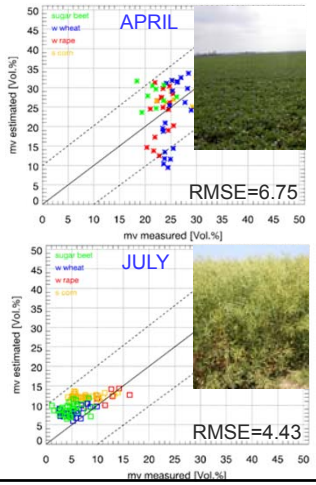

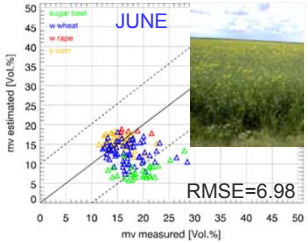

RMSE [vol.%]	APRIL	JUNE	JULY
sugar beet	7.55	11.90	4.68
winter wheat	8.06	6.15	3.40
winter rape	5.70	2.62	2.06
summer corn	5.34	3.20	5.25

validation box: 13x13 pixels

Slide 106

Summary Soil Moisture Estimation

- ***Soil moisture inversion is still object of scientific research:***
  - Main research focuses on the estimation of mv under the vegetation
  - One attempt is to use SAR polarimetry for scattering mechanism decomposition in order to characterise and subtract volume from a ground component (surface/dihedral)
  - PolSARPro provides the possibility to invert soil moisture over bare fields and allows a decomposition of scattering mechanisms
    - Outlook: Inversion procedures for vegetated areas are still missing

References (Part I)

Basic Text Books for SAR-Polarimetry and Pol-InSAR:

- **Cloude, S.,** Polarisation: application in remote sensing, Oxford University Press, p. 352, 2009.
- **Boerner, W. M. et al.,** 'Polarimetry in Radar Remote Sensing: Basic and Applied Concepts', Chapter 5 in F. M. Henderson, and A.J. Lewis, (ed.), "Principles and Applications of Imaging Radar", vol. 2 of Manual of Remote Sensing, (ed. R. A. Reyerson), Third Edition, John Willey & Sons, New York, 1998.
- **Elachi, C. & Van Zyl, J. J.,** 'Introduction to the physics and techniques of Remote Sensing', John Wiley and Sons, p. 552, 2006.
- **Lee, J.S. & Pottier, E.** 'Polarimetric Radar Imaging: From Basics to Aapplications', CRC Press, 2009.
- **Woodhouse, I.**, 'Introduction to Microwaves Remote Sensing', CRC Taylor & Francis, p. 370, 2005.

References (Part II)

Surface Parameter Inversion:

- Hajnsek, I., Pottier, E. & Cloude, S.R., 'Inversion of Surface Parameters from Polarimetric SAR', *IEEE Transactions on Geoscience and Remote Sensing*, vol. 41, no. 4, pp. 727-745, 2003.
- Lee, J.-S., Boerner, W.-M., Ainsworth, T. L., Hajnsek, I., Papathanassiou, K.P., Lüneburg, E., 'A Review of Polarimetric SAR Algorithms and their applications', Journal of Photogrammetry and Remote Sensing, vol. 9, No. 3, pp. 31-80, 2004.
- Hajnsek, I. & Cloude, S., 'The Potential of InSAR for Quantitative Surface Parameter Estimation' Can. J. Remote Sensing, vol. 31, no.1, pp. 85-102, 2005
- Hajnsek, Irena; Jagdhuber, Thomas; Schön, Helmut; Papathanassiou, Kostas (2009): Potential of Estimating Soil Moisture under Vegetation Cover by means of PolSAR. IEEE [Hrsg.]: IEEE Transactions on Geoscience and Remote Sensing, IEEE, vol 47, no 2, pp. 442 – 454.
- M. Arii, J.J. van Zyl and Y. Kim: A general characterization for polarimetric scattering from vegetation canopies, IEEE Transactions on Geoscience and Remote Sensing, vol. 48, pp. 3349-3357, 2010.
- M. Neumann and L. Ferro-Famil: Extraction of particle and orientation distribution characteristics from polarimetric SAR data, in Proc. of 8th European Conference on Synthetic Aperture Radar, June 7-10, 2010, Aachen, Germany, VDE, pp. 422-425.
- Jagdhuber, T., I. Hajnsek, A. Bronstert & K.P. Papathanassiou, 'Soil Moisture Estimation under Low Vegetation Cover Using a Multi-Angular Polarimetric Decomposition', *IEEE Transactions on Geoscience and Remote Sensing*,10.1108/TGRS.2012.2209433, p. 1-15, 2012.
- Jagdhuber, T. , I. Hajnsek, K.P. Papathanassiou, & A. Bronstert, 'Soil Moisture Retrieval Under Agricultural Vegetation Using Fully Polarimetric SAR', *Proc. of IEEE International Geoscience and Remote Sensing Symposium*, Munich, Germany, July 22-27, pp. 1481-1484 , 2012.
- Jagdhuber, T., 'Soil Parameter Retrieval under Vegetation Cover Using SAR Polarimetry, *PhD Thesis*, University Potsdam, Potsdam, supervised by Prof. Hajnsek and Prof. Bronstert, Date of Defense: 05.07.2012, http://nbn-resolving.de/urn:nbn:de:kobv:517-opus-60519, 2012.
- Bronstert, A., C. Creutzfeldt, T. Gräff, I. Hajnsek, M. Heistermann, S. Itzerott, T. Jagdhuber, D. Kneis, E. Lück & D. Reusser, 'Potentials and constraints of different type of soil moisture observations for flood simulations in headwater catchments', *Natural Hazards*, Vol. 60, pp.879–914 , 2012.

Acknowledgement to the AgriSAR Team

06/06/06

Acknowledgement to the OPAQUE Team

Slide 111

Part II: Exercises with L-band Airborne Data

- Read the airborne SAR data
- Speckle Filtering (refined Lee)
- Oh, Dubois and X-Bragg Inversion

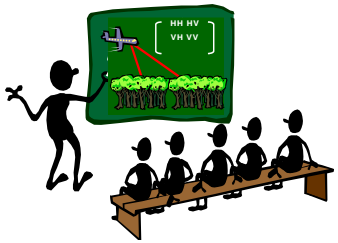

Slide 112

Test Date Used for the Exercise

- **Testsite: Demmin**
  - Location: Northern Germany
  - Acquisition Date: May 2012
  - Frequency: L-band
  - Data size: az: 2.75km rg: 2.2 km
  - Polarisation: 4 SLC
  - Resolution: az: 60cm x rg: 3.8m
  - Rows and colums: 7981 x 1837

Pauli RGB

Slide 113

First Steps in PolSARPro

- Please open PolSARPro
- Define your environment
- Open the DLR's acquired test Radar data

Slide 114